

PAPER

Shape coexistence in neutron-rich nuclei

To cite this article: A Gade and S N Liddick 2016 *J. Phys. G: Nucl. Part. Phys.* **43** 024001

Manuscript version: Accepted Manuscript

Accepted Manuscript is “the version of the article accepted for publication including all changes made as a result of the peer review process, and which may also include the addition to the article by IOP Publishing of a header, an article ID, a cover sheet and/or an ‘Accepted Manuscript’ watermark, but excluding any other editing, typesetting or other changes made by IOP Publishing and/or its licensors”

This Accepted Manuscript is© .



During the embargo period (the 12 month period from the publication of the Version of Record of this article), the Accepted Manuscript is fully protected by copyright and cannot be reused or reposted elsewhere.

As the Version of Record of this article is going to be / has been published on a subscription basis, this Accepted Manuscript will be available for reuse under a CC BY-NC-ND 3.0 licence after the 12 month embargo period.

After the embargo period, everyone is permitted to use copy and redistribute this article for non-commercial purposes only, provided that they adhere to all the terms of the licence <https://creativecommons.org/licenses/by-nc-nd/3.0>

Although reasonable endeavours have been taken to obtain all necessary permissions from third parties to include their copyrighted content within this article, their full citation and copyright line may not be present in this Accepted Manuscript version. Before using any content from this article, please refer to the Version of Record on IOPscience once published for full citation and copyright details, as permissions may be required. All third party content is fully copyright protected, unless specifically stated otherwise in the figure caption in the Version of Record.

View the [article online](#) for updates and enhancements.

Manuscript version: Accepted Manuscript

The “**Accepted Manuscript**” is the author’s original version of an article including any changes made following the peer review process but excluding any editing, typesetting or other changes made by IOP Publishing and/or its licensors.

During the embargo period (the 12 month period from publication of the Version of Record of this article), the Accepted Manuscript:

- is fully protected by copyright and can only be accessed by subscribers to the journal;
- cannot be reused or reposted elsewhere by anyone unless an exception to this policy has been agreed in writing with IOP Publishing



As the Version of Record of this article is going to be/has been published on a subscription basis, this Accepted Manuscript will be available for reuse under a [CC BY-NC-ND 3.0](#) licence after a 12 month embargo period.

After the embargo period, everyone is permitted to copy and redistribute this article for Non-Commercial purposes only, provided they*:

- give appropriate credit and provide the appropriate copyright notice;
- show that this article is published under a CC BY-NC-ND 3.0 licence;
- provide a link to the CC BY-NC-ND 3.0 licence;
- provide a link to the Version of Record;
- do not use this article for commercial advantage or monetary compensation; and
- only use this article in its entirety and do not make derivatives from it.

*Please see CC BY-NC-ND 3.0 licence for full terms.

View the Version of Record for this article online at iopscience.org

Shape coexistence in neutron-rich nuclei

A. Gade^{1,2} and S. N. Liddick^{1,3}

¹ National Superconducting Cyclotron Laboratory, Michigan State University, East Lansing, MI 48824 Michigan, USA

² Department of Physics and Astronomy, Michigan State University, East Lansing, 48824 Michigan, USA

³ Department of Chemistry, Michigan State University, East Lansing, 48824 Michigan, USA

Abstract. Shape coexistence in neutron-rich nuclei in the $N = 20$ island of inversion, along the $N = 28$ isotone line, and in the region around neutron number $N = 40$ is reviewed. The present status, emerging experimental opportunities and challenges in the interpretation are discussed.

1. Introduction

In neutron-rich nuclei, shape and configuration coexistence, where excitations across a shell gap become energetically favored and compete with normal-order configurations at low excitation energy [1], accompany shell evolution in the exotic regime. The resulting intruder states may exhibit collectivity and shape characteristics significantly different from neighboring states that are composed of normal-order configurations. Their properties provide unique information on the driving forces that fuel changes to the nuclear structure of rare isotopes. Their experimental and theoretical study is critical in the quest for a comprehensive understanding of nuclei.

In even-even nuclei, particularly fascinating and experimentally challenging are 0^+ states at low excitation energy. When these 0^+ states are sufficiently low in energy, so that $0^+ \rightarrow 0^+$ transitions are the only energetically allowed decay mode, conversion electron spectroscopy, the detection of internal pair formation, or the population and direct identification of these states with particle spectroscopy techniques are the only means to probe their properties. These shape- or configuration-coexisting states play an important role in the quest for an understanding of changes to the nuclear structure in exotic nuclei.

The following sections review the recent pioneering discoveries of shape-coexisting 0^+ states in the $N = 20$ “island of inversion” and at $N = 28$ in ^{44}S , and discuss the recent wealth of information about shape- and configuration-coexistence phenomena in the Co, Ni and Cu isotopic chains around $N = 40$. The present experimental frontiers, future challenges and opportunities for theory are presented.

2. Shape coexistence in the island of inversion: $N=20$

On the nuclear chart, the territory of neutron-rich neon, sodium, and magnesium isotopes with neutron numbers $N \approx 20$, has provided much insight into the driving forces of shell evolution. In this region, the so-called “island of inversion” [2], neutron n -particle n -hole (np - nh) intruder configurations of $(sd)^{-n}(fp)^{+n}$ character gain “correlation energy” [3] with respect to the normal-order configurations and dominate the wave functions of low-lying states, including the ground states. This structural change, fueled largely by the spin-isospin parts of the nuclear force [4–7] and a narrowing $N = 20$ shell gap [8], constitutes the breakdown of $N = 20$ as a magic number. One of the early experimental indicators for the disappearance of the $N = 20$ shell closure in this region was an onset of deformation [9–11].

Already more than 20 years ago, the deformation in the island of inversion was explicitly framed in terms of shape coexistence [12]. Along the $N = 20$ isotone line, shape coexistence had been established for ^{38}Ar with the identification of a collective band built on top of an excited 0^+ state [13]. Its configuration was assigned to neutron 2-particle 2-hole ($2p$ - $2h$) character from its population in a $^{36}\text{Ar}(t,p)^{38}\text{Ar}$ transfer reaction [14]. The $N = 20$ isotones ^{32}Mg , at the heart of the island of inversion with a deformed ground state, and ^{34}Si , located at the northern border of the island with a spherical ground state, were proposed to have coexisting spherical and deformed structures, respectively. A picture of shape coexistence is broadly consistent with the shell-model interpretation of neutron particle-hole excitations from the sd into the fp shell, making up the deformed intruder configurations that are the hallmark of the island of inversion [2, 12]. Experimentally, it took about two decades to actually find the shape-coexisting spherical and deformed 0^+ states in ^{32}Mg [15], ^{34}Si [16], and ^{30}Mg [17], respectively (see Fig. 1).

2.1. At the heart of the island: Shape coexistence in ^{32}Mg

In 2010, the inverse-kinematics (t,p) neutron-pair transfer reaction was used to selectively populate and identify the 0_2^+ state in ^{32}Mg at the very low excitation energy of 1058(2) keV [15]. The (t,p) transfer measurement was performed at the REX-ISOLDE facility at CERN with a 1.8 MeV/u ^{30}Mg rare-isotope beam impinging on a Ti target loaded with radioactive tritium. The energy and angular distribution of the protons in the exit channel were measured with the Si detector array T-REX [15, 18]. Coincident γ -ray spectroscopy was performed with the Miniball germanium detector array [15]. The excitation energy spectrum of ^{32}Mg , as reconstructed from the measured protons, is reproduced in Fig. 2(a). Two modest-resolution peaks are visible, the lowest-energy peak corresponding to the ground state of ^{32}Mg and a second peak at 1083(33) keV excitation energy. The proton angular distributions of both states were shown to follow the characteristic shape of an angular-momentum transfer of $\Delta L = 0$ starting from the 0^+ ground state of ^{30}Mg [15]. This strongly indicated that both states populated through (t,p) in ^{32}Mg have spin 0.

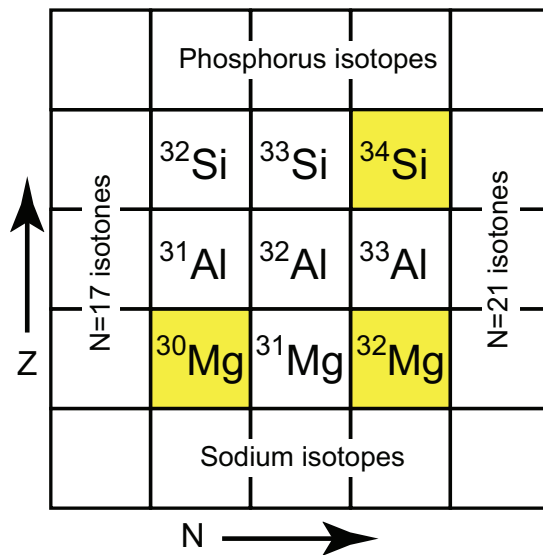


Figure 1. Region of the nuclear chart showing part of the $N = 20$ island of inversion. Shape coexistence in the nuclei highlighted in yellow will be discussed in the subsequent sections, ^{32}Mg at the heart of the "island" and ^{30}Mg and ^{34}Si at the isotopic and isotonic shores, respectively.

A γ -ray cascade detected in coincidence with the excited state, comprised of a new transition with an energy of 172 keV and the well-known $2_1^+ \rightarrow 0_1^+$ transition at 886 keV, put the newly-established excited 0^+ state at a more precise excitation energy of 1058(2) keV. Considering only normal-order and $(sd)^{-2}(fp)^{+2}$ configurations, cross-section calculations based on the DWBA formalism were used to infer that the ground state indeed carries $(f_{7/2})^2$ and $(p_{3/2})^2$ intruder configurations, while the cross section to the excited 0^+ state was found consistent with the assumption of sd -shell normal-order configurations, like $(d_{5/2})^2$, however, with a small $(p_{3/2})^2$ intruder contribution [15]. These findings were interpreted as supporting the picture of a deformed fp -shell intruder ground state and an sd -shell dominated, spherical, first excited 0^+ state. The approximately equal cross sections for the formation of the two 0^+ states in (t, p) point to substantial mixing between the two states. A measurement of the electric monopole strength connecting the two state is needed to quantify this aspect but could not be accomplished in the described experiment [15]. The 0_2^+ excitation energy of about 1 MeV was found significantly below available model predictions at the time [15]. The suggested shape coexistence in ^{32}Mg poses a formidable challenge for beyond-mean-field models with the calculations by Rodríguez-Guzmán *et al.* predicting a prolate-deformed ground state and a shape-coexisting spherical 0^+ state at significantly higher energy than experiment [19] and the model by Péru *et al.* [20] not reproducing the emerging picture of shape coexistence for ^{32}Mg .

Only recently, shell-model calculations that allow for the mixing of configurations that have 2, 4 and 6 neutrons promoted from the sd shell into the fp shell (SDPF-U-MIX effective interaction) reproduce the reported experimental 0_2^+ energy within about

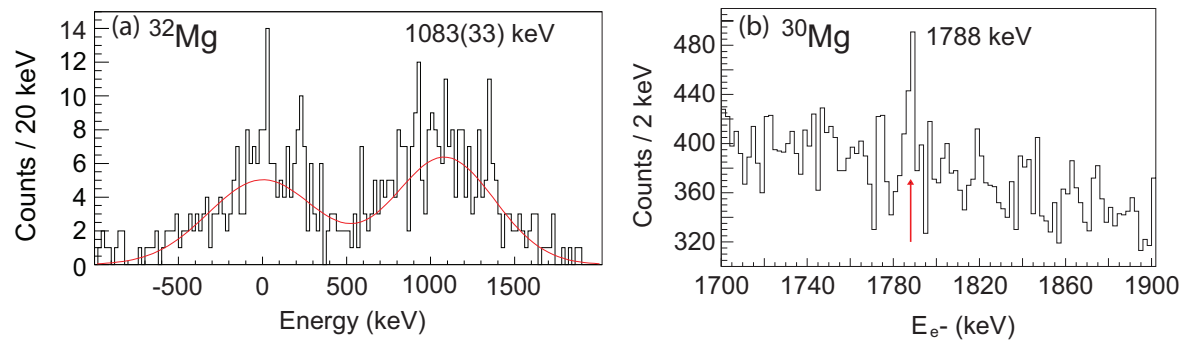


Figure 2. (a) Excitation energy spectrum of ^{32}Mg as reconstructed from the protons following the (t, p) transfer. Both peaks showed a proton angular distribution commensurate with an angular-momentum transfer of $\Delta L = 0$ [15], putting the 0_2^+ state just above 1 MeV. (b) Conversion-electron spectrum detected following the β decay of ^{30}Na to ^{30}Mg , establishing the second 0^+ state of ^{30}Mg at 1788 keV. Figures reprinted from [15] and [17]. Copyrighted by the American Physical Society, 2010 and 2009.

200 keV and suggest rather exceptional character for the 0^+ states of ^{32}Mg [21]. The ground-state neutron configuration is calculated to 9% 0p-0h, 54% 2p-2h, 35% 4p-4h, and 1% 6p-6h and thus is a mixture of deformed and superdeformed configurations [21]. The excited 0^+ state is predicted to carry 33% 0p-0h, 12% 2p-2h, 54% 4p-4h, and 1% 6p-6h neutron particle-hole configurations, painting a rather complex picture of ^{32}Mg where the second 0^+ state is comprised of large spherical as well as superdeformed configurations [21], rendering the simple concept of a deformed ground state and a spherical excited 0^+ as too simplistic. From an experimentalist's point of view, the confirmation and further characterization of the very interesting 0_2^+ state of ^{32}Mg , like the measurement of its lifetime and the identification of structures built on top, appears necessary to guide a quantitative understanding of the important phenomenon of shape coexistence inside the $N = 20$ "island of inversion".

2.2. At the northern and western shores: ^{34}Si and ^{30}Mg

At the shores of the "island of inversion", excited deformed intruder configurations will coexist with the still spherical ground states. To date, shape-coexisting 0^+ states have been identified in ^{34}Si [16] and ^{30}Mg [17].

Along the line of the $N = 20$ isotones, ^{34}Si is situated at the northern boundary of the island of inversion. Some basic indicators, a high-lying first excited 2^+ state and a corresponding low $B(E2; 0^+ \rightarrow 2^+)$ electromagnetic excitation strength hint at a spherical ground state and the presence of the $N = 20$ shell gap for ^{34}Si [22]. With strongly-deformed ^{32}Mg only two protons south, one may expect to find a deformed 0^+ state, dominated by neutron fp -shell configurations, at modest excitation energy, possibly below the high-lying 2_1^+ state. In a dedicated measurement at GANIL, the β decay from a 1^+ isomer of ^{34}Al was used to selectively populate 0^+ states in

^{34}Si , including for the first time the excited 0_2^+ state at 2719(3) keV, indeed located below the 2_1^+ state [16]. Since γ -ray decays between 0^+ states are angular-momentum forbidden, the excited 0^+ state can only decay via electron conversion or internal pair formation (IPF), where an electron-positron e^+e^- pair is emitted with an energy of $E_{e^-} + E_{e^+} = E(0_2^+) - 2 \times 511$ keV. Rotaru *et al.* used Si-Si(Li) telescopes for the electron/positron spectroscopy and found, when correlating the total electron/positron energy detected in one telescope versus a second, events for which the energy detected in the two telescopes sums to a peak at $E_{e^+} + E_{e^-} = 1688(2)$ keV [16]. When applying a small energy-loss correction of 9(1) keV, this establishes the first excited 0^+ state of ^{34}Si to $E(0_2^+) = 2719(3)$ keV [16]. From the time difference measurement between the β events and the e^+e^- pair detection, a half-life of 19.4(7) ns could be deduced for the 0_2^+ state [16] (reprinted in Fig. 3). The extracted low $E0$ transition strength indicates only weak mixing between the two 0^+ states and all spectroscopic information together with $B(E2; 2_1^+ \rightarrow 0_2^+) = 61(40)e^2\text{fm}^4$, as deduced from a small γ -ray branch and the 2^+ lifetime, suggest a quadrupole deformation parameter of $\beta = 0.29(4)$ for the 0_2^+ state, in agreement with large-scale shell-model calculations that allow for neutron 2p-2h excitations across the $N = 20$ shell gap [16].

Approaching ^{32}Mg along the chain of $Z = 12$ isotopes, shape coexistence was proven in ^{30}Mg through the identification of the first excited 0^+ state via its electric monopole transition to the ground state [17]. The measured small $E0$ transition strength was interpreted as evidence for two competing configurations with largely different quadrupole deformation, again strongly supporting the picture of shape coexistence in the island of inversion.

From early fast-timing work, an excited state at 1789 keV had emerged as a candidate for the 0_2^+ state in ^{30}Mg from its lifetime of several nanoseconds and the absence of a γ -ray decay to the ground state [23]. The proof came from an experiment at ISOLDE where ^{30}Mg was populated in the β decay of ^{30}Na [17]. The decay parent was stopped in an Al foil. Electron spectroscopy was performed with liquid-nitrogen-cooled Si(Li) detector in conjunction with a “miniorange” magnetic transport and focusing system based on permanent magnets [17]. In delayed coincidence with β particles, a peak in the electron spectrum at 1788 keV (reprinted in Fig. 2(b)), stemming from the $0_2^+ \rightarrow 0_1^+$ $E0$ conversion-electron transition, was measured. From the partial lifetime, a weak $E0$ transition strength was deduced [17]. In a shape-coexistence picture, a small $E0$ transition strength indicates weak coupling between the two potential minima. Within a two-state mixing approach, assuming that the 0^+ states have competing normal-order sd -shell and intruder fp -shell configurations, a small value for the $E0$ strength translates into rather pure sd and fp configurations for the two 0^+ states [17]. From this measurement alone, it cannot be deduced if the ground state or the excited 0^+ state are of intruder nature. However, there are complementary experimental signatures, $B(E2)$ values [24, 25] and spectroscopic factors [26], that strongly indicate that an inversion has not taken place for ^{30}Mg and the spherical configuration is most likely the ground state with a deformed intruder 0_2^+ excited state [17]. In fact, root-mean-squared charge-radii

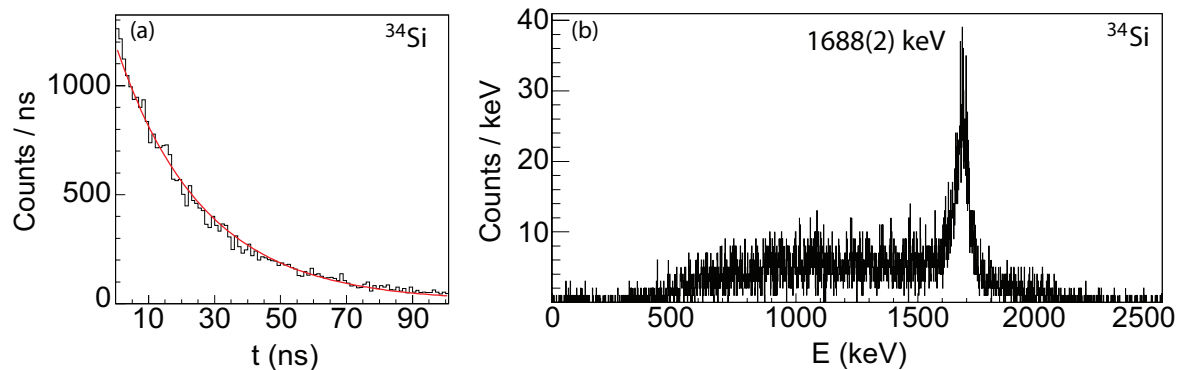


Figure 3. (a) 0_2^+ excited-state lifetime, $\tau = 19.4(7)$ ns, as deduced from the time distribution between β trigger and e^+ or e^- detection [16]. (b) Example spectrum showing the sum of the total energy $E_{e^+} + E_{e^-}$ detected in two Si-Si(Li) telescopes, with background removed through event selection 16 ns after the β trigger and a multiplicity above three [16]. This allows for the extraction of $E(0_2^+) = E_{e^-} + E_{e^+} + 2 \times 511$ keV (not taking into account small energy-loss corrections). Figures reprinted from [16]. Copyrighted by the American Physical Society, 2012.

measurements for $^{21-31}\text{Mg}$ performed at ISOLDE [27] show a change in slope for the root-mean-squared charge radius $\langle r^2 \rangle^{1/2}$ vs. neutron number starting at ^{31}Mg , strongly suggesting that starting at ^{31}Mg neutron fp shell orbitals are being filled, placing the western border of the island of inversion between ^{30}Mg and ^{31}Mg [27].

The newest shell-model calculations based on the SDPF-U-MIX effective Hamiltonian [21], that allow for mixing of neutron np - nh excitations and that propose the aforementioned exceptional structure for the 0^+ states of ^{32}Mg , support the picture of ^{30}Mg and ^{34}Si having ground states which are more than 80% dominated by neutron $0p$ - $0h$ nature and first excited 0^+ states with dominant neutron $2p$ - $2h$ character [21]. For both cases at the shores of the island, the experimental challenge is the identification and characterization of deformed structures on top of the intruder 0^+ states to probe their configurations.

3. Shape and configuration coexistence along $N = 28$: S, Si, and Mg

Like for the breakdown of $N = 20$ in the island of inversion, studies of the magic neutron number $N = 28$ and of its fate in the neutron-rich regime have advanced the field in the quest for unraveling the driving forces of shell evolution. Also, 28 is the first magic number that requires a strong spin-orbit interaction. South of doubly magic $^{48}\text{Ca}_{28}$, the stabilizing effect of the $N = 28$ shell gap was shown to vanish progressively in $^{44}\text{S}_{28}$ [28] and $^{42}\text{Si}_{28}$ [29], both displaying strong indicators of collectivity or deformation rather than closed-shell character.

Early on, similar to the $N = 20$ isotonic chain, shape changes were predicted along the $N = 28$ isotone line between spherical ^{48}Ca and well-deformed ^{42}Si [30, 31]. In between these two extremes lies ^{44}S , for which the coexistence of deformed and

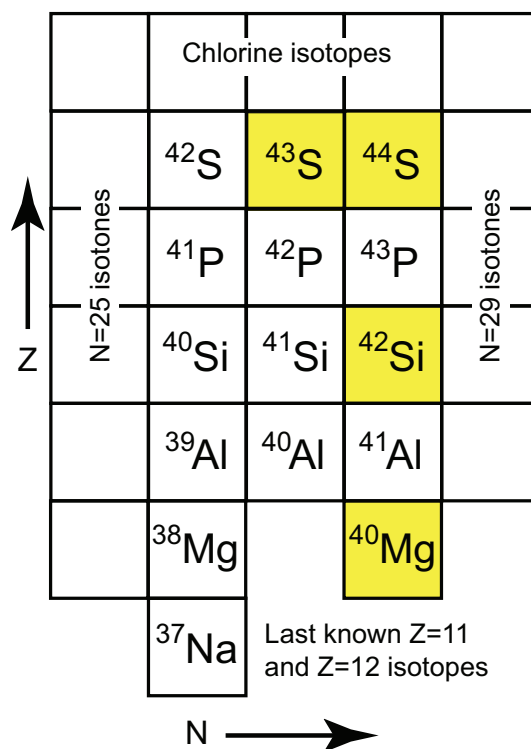


Figure 4. Section of the nuclear chart around the $N = 28$ isotone line. Shape-coexistence studies in the nuclei highlighted in yellow will be reviewed in the following subsections.

spherical shapes at low excitation energy is expected. The collective nature of ^{44}S was concluded early on from its low-lying 2_1^+ state and its high $B(E2)$ quadrupole excitation strength [28]. The $N = 28$ isotones ^{42}Si and ^{40}Mg are predicted to exhibit shape-coexistence as well, however, likely eluding experimental proof until next-generation rare-isotope facilities come online. The nuclei that will be discussed in the following are highlighted in Fig. 4.

3.1. Shape changes in the sulfur isotopes

Around 2005, the lowest-lying excited 0^+ state of ^{44}S was first identified at GANIL to lie at 1365 keV [32], just 36 keV above the first 2^+ state. The ^{44}S nuclei were produced in the projectile fragmentation of a ^{48}Ca primary beam and implanted into a kapton foil. A fraction of the ^{44}S was produced in the excited 0^+ state which turns out to be long-lived with a half-life exceeding $2 \mu\text{s}$ [32]. Electron spectroscopy with Si(Li) detectors then allowed to measure the delayed conversion electrons that signal the $0_2^+ \rightarrow 0_1^+$ $E0$ transition. This important measurement was repeated at GANIL by the same group with more statistics and an improved experimental setup that allowed an extraction of the transition probability $B(E2; 2_1^+ \rightarrow 0_2^+)$ [33]. The electron spectrum showing the internal-conversion electron decay at an energy of 1362.5(10) keV is reprinted in Fig. 5. The time distribution of the conversion-electron events relative to implantation

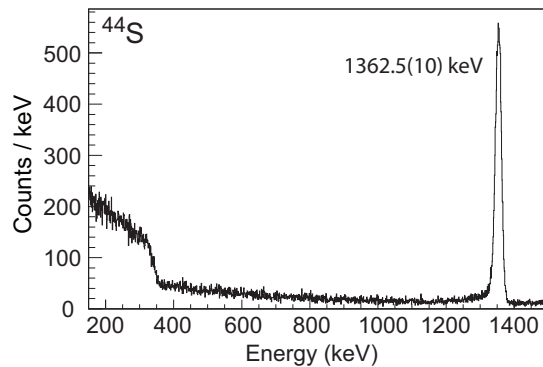


Figure 5. Electron spectrum as measured with the Si(Li) detectors of [33]. The peak at 1362.5 keV originates from the $0_2^+ \rightarrow 0_1^+$ $E0$ transition. The enhancement at low energies stems from IPF, where the e^+e^- pair carries $E_{e^+} + E_{e^-} \approx 340$ keV [33]. Reprinted from publication [33]. Copyrighted by the American Physical Society (2010).

revealed a half-life of $2.619(26)$ μs for the 0_2^+ state [33]. The resulting $E0$ strength together with the $B(E2; 2_1^+ \rightarrow 0_2^+)$ transition strength and a two-state mixing approach hint at weak mixing between the two 0^+ states with a (prolate) deformed 0^+ ground state ($\beta \approx 0.25$) and a near-spherical excited 0_2^+ state, in agreement with large-scale shell-model calculations [33]. This result provides a critical benchmark for nuclear structure theory in the quest to model the rapid shape and shell evolution taking place along the $N = 28$ isotone line.

The broader context of configuration coexistence has been discussed recently for ^{44}S , based on results from an excited-state lifetime measurement performed at NSCL [34]. Excited states in ^{44}S were populated in the two-proton removal from a ^{46}Ar secondary beam produced at the A1900 fragment separator. The reaction target was located at the target position of the S800 spectrograph and was surrounded by the segmented germanium detector array SeGA. In coincidence with ^{44}S detected in the S800 spectrograph, a γ -ray transition depopulating a low-lying, presumably the first, 4^+ state, was identified and showed a lineshape indicative of a mean lifetime of around 50 ps [34]. This indicates that the proposed 4_1^+ state has a surprisingly hindered $E2$ transition to the first 2^+ state with a transition strength of $\lesssim 1$ W.u. [34]. This is highly unusual as $E2$ decays connecting yrast states typically proceed with tens to hundreds of Weisskopf units of transition strength. A shell-model calculation using the SDPF-U interaction suggested that this 4^+ state has a strong prolate deformation in the laboratory and intrinsic frames, but that its deformation is based on a neutron 1p-1h configuration, differing from the neutron 2p-2h intruder configuration responsible for the ground-state deformation of this nucleus [34]. Recent calculations by Utsuno *et al.* that used a variation-after-angular-projection approximation to shell-model calculations (with the SDPF-MU effective interaction) suggest the first 4^+ state of ^{44}S to be a triaxially deformed $K = 4$, isomer [35]. This highlights the pivotal role of ^{44}S on the path from spherical ^{48}Ca to well-deformed ^{42}Si .

Relativistic mean field calculations for ^{44}S , see for example [36], and beyond-mean-field studies with the Gogny functionals, e.g. [19, 37], show the breakdown of the $N = 28$ shell closure already at the mean-field level and predicted admixtures of triaxial configurations, and shape coexistence. A complementary interpretation is given in [38] where configuration-mixing methods on top of beyond-mean-field calculations are qualitatively consistent with the spectroscopic data, however, attributing the observations to broad configuration mixing rather than shape coexistence and with a $K = 4$ 4^+ state beyond 5 MeV rather than at very low energy. The magnitude and sign of the quadrupole moments of low-lying excited states of ^{44}S , as accessible through low-energy Coulomb excitation, would provide important experimental clarification.

Already in 2000, an isomer was discovered at 320 keV excitation energy in neighboring ^{43}S in a time-of-flight mass measurement performed at GANIL [39] and suggested to be a shape isomer. In comparison to shell-model calculations, the hindered transition was attributed to very different wave functions and deformation of the isomer and the ground state [39]. A g -factor measurement almost a decade later proved the isomer to have angular momentum and parity $7/2^-$ and suggested it to be built on the normal-order $f_{7/2}^{-1}$ neutron-hole configuration, which – together with neutron $p_{3/2}$ intruder nature of the ground state – underlines the erosion of the $N = 28$ shell gap [40].

A shell-model interpretation of the previously mentioned results suggests shape coexistence with the normal-order $7/2^-$ isomer and the supposedly prolate-deformed intruder ground state within less than 400 keV in ^{43}S [40]. The spectroscopic quadrupole moment of the $7/2^-$ isomer was finally measured in 2012 using the time dependent perturbed angular distribution technique at the RIKEN RIBF facility [41], providing first quantitative and direct information on the shape of the $7/2^-$ isomer. The spectroscopic quadrupole moment of $|Q_s| = 23(3)$ efm² was found to be significantly larger than expected for a pure single-particle state and neutron-intruder configurations, driven by proton-neutron correlations, are suggested to contribute to the wave function of the $7/2^-$ isomer [41].

The next experimental challenges are the characterization of the excited 0^+ state of ^{44}S through excitations built on top, measurements of the magnitude and the sign of the quadrupole moments of low-lying states in ^{44}S , and the identification of a rotational structure built on the supposedly prolate-deformed ground state of ^{43}S .

3.2. Challenges south of ^{44}S : Changing shapes in ^{42}Si and ^{40}Mg

Further south along the $N = 28$ isotone line, changing shapes and shape coexistence are predicted, most recently from large-scale shell-model calculations with the SDPF-U [42] and the SDPF-MU [43] effective interactions. Both Hamiltonians characterize ^{42}Si as having a strongly oblate-deformed ground state. The shape and deformation of the neutron-rich silicon isotopes was tied explicitly to the action of the tensor force in the work of Utsuno *et al.* [43]. While some of the characteristics of the two shell-model Hamiltonians are very similar, in particular for the known spectroscopy, Tostevin,

Brown, and Simpson point out dramatic differences that are manifested in low-lying 0^+ states of ^{42}Si [44]. Considering the two-proton removal reaction from ^{44}S to ^{42}Si , marked differences in the level schemes became apparent through the calculated final-state cross sections that combine reaction theory and shell-model wave function overlaps [44]. In fact, the spectroscopy of ^{42}Si may serve to discriminate the two shell-model effective interactions at the key $N = 28$ magic number. The final states that are predicted to be populated in ^{42}Si following the direct two-proton removal reveal three excited 0^+ states below 2.4 MeV with the SDPF-U effective interaction, while the SDPF-MU Hamiltonian predicts the first excited 0^+ state only at 2.57 MeV [44]. The populations of these discriminatory 0^+ states are calculated to be non-negligible in both scenarios, holding promise for an answer through experiment.

The spectroscopy of ^{42}Si has been a challenge for many years [45, 46] and was accomplished first at GANIL [29] and subsequently at RIBF/RIKEN [47]. In all cases, the two-proton removal from ^{44}S to ^{42}Si was used as population mechanism for excited states. A high-resolution, modest-efficiency measurement at NSCL failed [45, 46], while the highest-statistics measurement performed at RIBF/RIKEN employed the modest-resolution, high-efficiency scintillator array DALI2 [47], not allowing for the detailed, high-resolution γ -ray spectroscopy required to identify the fingerprints of the dramatically differing shell-model level schemes beyond the yrast states. The first 2^+ energy of ^{42}Si was found to be the lowest in the region, signaling the development of strong collectivity [29]. No firm J^π assignments are available beyond the first 2^+ state [47]. For the future, the high-statistics, high-resolution spectroscopy of ^{42}Si , for example, using again the two-proton knockout from ^{44}S , seems to emerge as a key in refining the driving forces of shell evolution and their incorporation into nuclear models for the textbook example of $N = 28$.

The existence of the near-dripline nucleus ^{40}Mg was only established in 2007 [48] and a first attempt of its γ -ray spectroscopy following the two-proton removal reaction from a ^{42}Si projectile beam at RIBF/RIKEN failed due to low statistics [49]. However, the cross section for the reaction was measured and provides information on the wave function overlaps of the ground state of ^{42}Si and all bound final states of ^{40}Mg . Theoretical cross sections for two-proton knockout combine reaction theory and two-nucleon amplitudes from shell model [50]. Using the SDPF-U and SDPF-MU effective interactions, the small measured cross section of $\sigma = 40_{-17}^{+27}\mu\text{b}$ could only be explained if the first excited 0^+ state of ^{40}Mg , which is predicted to carry the dominant spectroscopic strength in the two-proton removal from ^{42}Si , is in fact neutron unbound [49]. Using the knockout cross section as a measure of the wave function overlap and assuming two-level (shape) mixing only, Crawford *et al.* interpret the small cross section as consistent with a structural mismatch between the oblate-deformed ^{42}Si ground state [42, 43] and a prolate deformed ^{40}Mg ground state [42] and with the shape-coexisting oblate-deformed excited 0^+ state of ^{40}Mg being above the neutron separation energy [49]. This interpretation is broadly consistent with the current shell-model picture [42, 43]. The detailed high-resolution spectroscopy of ^{40}Mg may have to wait for next-generation rare-isotope facilities to

come online.

4. Competing shapes along N=40 in the neutron-rich Ni isotopes and neighboring isotopic chains

The region around $Z \sim 28$ and $N \sim 40$ continues to elicit numerous experimental and theoretical inquiries. The properties of nuclei in this region depend on the size of the energy gaps at $Z = 28$ and $N = 40$ and the ease of exciting nucleons across the gaps. The gap at $Z = 28$ is defined by the energy separation between the $f_{7/2}$ and the rest of the pf shell while the $N = 40$ gap is between the neutron pf shell and the $g_{9/2}$ orbital. The magnitude of the energy gaps can vary as a function of both proton and neutron number. Within shell model calculations, the energy gap at $N = 40$ is gradually eroded away as protons are removed from the $\pi f_{7/2}$ single-particle state under the action of the tensor force [5, 51]. Progressing from ^{68}Ni to ^{60}Ca , the neutron $f_{5/2}$ orbital intrudes into the $N = 40$ energy gap until, at ^{60}Ca , it is almost degenerate with the $g_{9/2}$ single-particle state [52, 53]. The narrowing of the energy gap facilitates excitations into the deformation-driving neutron $g_{9/2}$ orbital. Likewise, the energy separation between the proton $f_{5/2}$ and $f_{7/2}$ single-particle states is reduced as neutrons are added to the $g_{9/2}$ orbital. However, a qualitatively different picture is encountered within beyond mean-field calculations regarding the energy separation between the $f_{5/2}$ and $g_{9/2}$ neutron single-particle orbitals. The difference between the two single-particle energies remains relatively constant around 3.9 MeV from $Z = 22 - 42$ [54].

In ^{68}Ni , the high excitation energy of the first excited 2^+ state, $E(2_1^+)$ [55], low $B(E2; 0_1^+ \rightarrow 2_1^+)$ value [56], and low-energy 0^+ state [55], all originally suggested a doubly-magic character for ^{68}Ni . However, that conjecture was not supported by later observables, such as the mass surface around $N = 40$ [57]. A rapid increase in collectivity is inferred from the drop in $E(2_1^+)$ values when moving away from ^{68}Ni in the even-even isotopes of Fe [58, 59], and Cr [60, 61]. Complementary lifetimes [62, 63], $B(E2)$ values [64, 65], as well as deformation lengths from proton scattering measurements [66], also support the rapid increase in collectivity.

The occupation of the deformation driving neutron $g_{9/2}$ orbital well before $N = 40$ was recognized early. Tentative $9/2^+$ states, many of which are isomeric, are observed in odd-A Cr [67] and Fe [68–70] nuclei. The influence of the $g_{9/2}$ orbital is also seen through the presence of decoupled positive-parity rotational bands in $^{55,57}\text{Cr}$ [71, 72]. Proton excitations out of the $f_{7/2}$ across $Z = 28$ have also been suggested to account for certain states in odd-A Cu [73, 74] and Co [75, 76]; only recently has a nearly complete set of systematics become available.

The large, computationally-costly, model space required to accommodate excitations across both the proton and neutron energy gaps at $Z = 28$ and $N = 40$ has traditionally resulted in the treatment of these nuclei in truncated spaces. Large-scale shell-model calculations in the $pf g_{9/2} d_{5/2}$ model spaces have become tractable over the past few years with both the LNPS [52] and A3DA [53] effective interactions, allowing

for a theoretical description of the rapid development of collectivity below ^{68}Ni .

The competition between the energy cost to promote a particle across the energy gap versus the energy gained from the proton-neutron interaction has the potential to stabilize excitations across the gaps and could lead to shape coexistence at low energies [1]. Theoretical calculations have suggested the possibility of shape coexistence for some nuclei in this region [54, 55, 77] and recent, large-scale shell-model calculations have identified coexisting structures in both Ni and Co isotopes [53, 78]. The experimental indications for shape coexistence in this region of the nuclear chart have come mainly from the study of the neutron-rich ^{27}Co , ^{28}Ni , and ^{29}Cu isotopes. This review is organized according to Z with discussions on the isotopes of Co in Sec. 4.1, Ni in Sec. 4.2, and Cu in Sec. 4.3. In all three sections, experimental data is presented which, when viewed systematically, suggests the presence of deformed configurations coexisting alongside the expected spherical states.

4.1. The Co isotopes

The ground state spin and parity of all odd- A Co isotopes up to $N = 40$ is tentatively assigned as $(7/2^-)$ based on the proton $f_{7/2}^{-1}$ configuration. The suggestion of multiple coexisting states in nuclei below Ni was initiated by the observation of a low-spin, isomeric, $(1/2^-)$ state in ^{67}Co , see Fig 6. The state was identified at 492 keV in the β -decay of ^{67}Fe by looking for γ -ray transitions delayed in time with respect to a known β -delayed γ -ray transition in ^{67}Co [75]. The low-energy of the $(1/2^-)$ state is naturally explained based on Nilsson orbitals [79]. For prolate deformations, the down-sloping orbitals for both protons (the $[321]1/2^-$ state originating from the $p_{3/2}$ spherical state) and neutrons (the $[440]1/2^+$ and $[431]3/2^+$ states originating from the $g_{9/2}$) are present. The deformation inferred for the $(1/2^-)$ state is $0.25 < \beta_2 < 0.4$ [75]. The low-energy of the $(1/2^-)$ state with respect to the $(7/2^-)$ ground state has been reproduced in large-scale shell-model calculations using the LNPS interaction [52], consisting of the pf shell for protons and the neutron $pf g_{9/2} d_{5/2}$ orbitals. These calculations associate the $(1/2^-)$ state with the excitation of four neutrons into the $g_{9/2} d_{5/2}$ orbitals, in addition to the excitation of a single proton out of the $f_{7/2}$ single-particle state. A rotational band is predicted on top of the calculated $(1/2^-)$ state with a large, constant intrinsic quadrupole moment of $Q_0 \sim 180 \text{ efm}^2$ [78]. A possible transition associated with this band was identified at 189 keV [75] but the spin and parity of the initial state is still uncertain [78].

Deformed intruder states have also been tentatively identified in the neighboring odd- A $^{65,69}\text{Co}$ nuclei. A $(1/2^-)$ state at 1095 keV was put forward as the intruder state in ^{65}Co [76] based on a lack of feeding in the β -decay of ^{65}Fe similar to the decay pattern in ^{67}Co . A $(3/2^-)$ level above the $(1/2^-)$ level in ^{65}Co is suggested as a rotational band member [75, 76]. In ^{69}Co , a β -decaying isomeric state has been detected based on differences in the absolute intensities of the β -delayed Ni γ rays depending on whether ^{69}Co was produced directly or as a daughter product in the β -decay of ^{69}Fe [80]. No

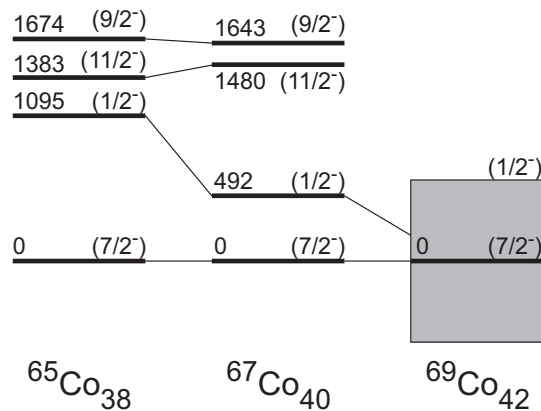


Figure 6. Tentative low-energy $7/2^-$, $1/2^-$, $9/2^-$ and $11/2^-$ states in the Co isotopes as a function of neutron number. The $9/2^-$ and $11/2^-$ levels follow the systematics of the 2_1^+ energies in the adjacent even-even Ni cores. The $1/2^-$ level is suggested to be a deformed intruder. The shaded gray area at for $^{69}\text{Co}_{42}$ indicates the range of possible excitation energies of the $1/2^-$ level relative to the $7/2^-$ state.

isomeric γ rays were observed following the tentatively identified ^{69}Fe β -delayed γ -rays. The relative energy difference between the tentative $7/2^-$ and $1/2^-$ states in ^{69}Co is estimated to be ~ 660 keV based on the non-observation of a γ -ray [81]. If the drop in excitation energy follows the trend observed in the neutron-rich Cu isotopes (detailed in Sec. 4.3), the deformed state could be the ground state configuration in ^{69}Co . Further experimental efforts are clearly warranted to identify which of the two β -decaying states is the ground state, in particular to determine whether the minimum in the intruder energy is located at $N = 42$ or $N = 44$. The systematic trend of the low-energy ($1/2^-$) levels in the neutron-rich $^{65,67,69}\text{Co}$ isotopes is presented in Fig. 6.

Coexisting alongside the ($1/2^-$) levels discussed previously, are states that would be naturally expected in the odd-A Co isotopes based on the coupling of a single proton hole in the $f_{7/2}$ orbital to the adjacent even-even Ni cores. The energy systematics of the $9/2^-$ and $11/2^-$ levels in the Co isotopes closely follow the excitation pattern of the adjacent 2_1^+ levels in the neighboring Ni cores. This supports the interpretation of the $9/2^-$ and $11/2^-$ levels as the $\pi f_{7/2}^{-1}$ proton coupled to the 2_1^+ excitation in the adjacent Ni isotopes [76, 78]. Lifetime measurements of the $11/2^-$ result in a close match between the $B(E2; 11/2^- \rightarrow 7/2^-)$ in $^{63,65}\text{Co}$ and the corresponding Ni $B(E2; 0^+ \rightarrow 2^+)$ values [82], further supporting such an interpretation. Lifetime results for the $9/2^-$ level in ^{63}Co , assuming a pure E2 transition, result in a $B(E2; 9/2^- \rightarrow 7/2^-)$ value which is also compatible with the $B(E2; 0^+ \rightarrow 2^+)$ in ^{64}Ni [83].

4.1.1. Isotopic chains lighter than Ni The further one progresses from the Ni isotopes, the harder it is to interpret existing experimental data. Still, some evidence exists in lighter nuclei to support shape coexistence in this region. The existing yrast bands of the neutron-rich $^{62,64,66,68}\text{Fe}$ and $^{60,62,64}\text{Cr}$ nuclei have been interpreted based on a mixing

between coexisting “spherical” and “deformed” configurations [84]. The yrast structure of ^{60}Fe has been observed up to high spin ($20\hbar$). Plotting the spin of the state versus $\hbar\omega$ displays a clear backbending behavior due to the crossing of two yrast bands. One band belongs to the expected shell-model configuration of neutrons in the pf shell and another is associated with a pair of particles in a rotational band built on an aligned $g_{9/2}^2$ neutron configuration with a prolate-deformed shape. The yrast states of ^{60}Fe up to the 6^+ are well described by shell-model calculations without needing to invoke excitations into the $\nu g_{9/2}$ orbital while that is not the case for the levels between 8^+ and 20^+ .

The yrast sequence of ^{60}Fe was used as a template for two-band mixing calculations between shell-model and deformed states [84]. The shell-model states were calculated using the GXPF1A interaction [85], in which particles are restricted to the pf shell. The deformed states were determined based on a rotational model using the energy separation between the 2^+ and 0^+ states. An interaction strength of 100 keV was assumed for the mixing between states for all nuclei investigated. The best match with experimental data was then determined by varying only the energy of the deformed 0^+ state. The deformed structures drop from an energy of 2.4 MeV in ^{60}Fe to approximately 300 keV near $N = 40$. While mixing is present, the predominate configuration for the ground state is spherical in the Fe isotopes and deformed in the Cr isotopes. This change in the nature of the ground states could explain differences in knockout reaction cross sections along an isotonic chain [61]. The existence of rotational band structures with deformed quadrupole shapes have also been observed at high spins in numerous nuclei, including $^{56,57,58,59,60,63}\text{Ni}$ and ^{61}Co (see, for example, the work on ^{61}Co [86] and ^{63}Ni [87] and references, therein).

4.2. The Ni isotopes

A wealth of new information on the the neutron-rich Ni isotopes has been obtained in the last few years. The level schemes of $^{64,66,68}\text{Ni}$ have been clarified [88] and new levels have been identified through β -decay [89, 90], single-nucleon transfer [91], multi-nucleon transfer [88, 92–95] and knockout reactions [93].

4.2.1. 0^+ states The presence of low-energy 0^+ states in even-even nuclei is one signature of shape coexistence [1]. The systematics of the lowest three 0^+ states (when known) for the neutron-rich $^{64,66,68,70,72}\text{Ni}$ isotopes are given in Fig. 7. The originally reported 0_2^+ level at 1770 keV in ^{68}Ni , identified in heavy-ion transfer reactions [55], has been remeasured and placed at an energy of 1604 keV based on the direct detection of the $0_2^+ \rightarrow 0_1^+$ electric monopole transition [89]. The state has also been indirectly observed through its delayed 511-keV radiation following the internal pair-production decay of the isomeric 0_2^+ state in both multi-nucleon transfer and high-energy knockout reactions [93]. Shell-model calculations in restricted spaces [93] as well as calculations using the LNPS [52] and A3DA [53] effective interactions are all successful in reproducing the energy of the 0_2^+ state. The wave function of the 0_2^+ state contains a dominant component

$\frac{3026}{2867} \begin{matrix} 0^+ \\ 0_2^+ \end{matrix}$	$\frac{2671}{2443} \begin{matrix} 0^+ \\ 0_2^+ \end{matrix}$	$\frac{2511}{1604} \begin{matrix} 0^+ \\ 0_2^+ \end{matrix}$	$\frac{1567}{1567} \begin{matrix} 0^+ \\ 0_2^+ \end{matrix}$
$\frac{0}{64} \begin{matrix} 0^+ \\ \text{Ni}_{36} \end{matrix}$	$\frac{0}{66} \begin{matrix} 0^+ \\ \text{Ni}_{38} \end{matrix}$	$\frac{0}{68} \begin{matrix} 0^+ \\ \text{Ni}_{40} \end{matrix}$	$\frac{0}{70} \begin{matrix} 0^+ \\ \text{Ni}_{42} \end{matrix}$

Figure 7. Known low-energy excited 0^+ states in neutron-rich Ni isotopes. Data taken from [88, 92, 94].

associated with the excitation of a pair of neutrons across $N = 40$ into the $\nu g_{9/2}$ orbital [89, 93, 96].

The wave functions of the low-energy levels in numerous neutron-rich nuclei, starting with ^{68}Ni , were characterized according to their intrinsic deformations using the A3DA interaction in the Monte Carlo shell model (MCSM) [53, 97]. The values of Q_0 and Q_2 were determined for each component of the wave function and located on a corresponding potential energy surface. The distribution of Q_0 and Q_2 for each component of the wave function, and the magnitude of its overlap with the total wave function, provides information on the intrinsic shape of each level. In this manner, the 0_1^+ ground state was associated with a spherical shape and the 0_2^+ level was suggested to be slightly oblate. Assuming an axially symmetric deformation, maximal mixing, and taking one of the two 0^+ states to be spherical, the electric monopole transition strength, $\rho^2(E0)$, between the 0_2^+ and 0_1^+ states resulted in an absolute value for the difference in intrinsic quadrupole moments which is consistent with the MCSM theoretical calculations of $\sim -95 \text{ efm}^2$ [89].

A 0^+ state associated with proton excitations is also expected in ^{68}Ni . The energy of the state was predicted at 2.2 MeV based on a summing prescription involving the suspected proton one-particle, two-hole and two-particle, one-hole configurations in neighboring ^{67}Co and ^{69}Cu , respectively [98]. Shell-model calculations within restricted model spaces that do not explicitly allow for proton excitations out of the $f_{7/2}$ orbital are unable to place a third 0^+ state below 3 MeV [93]. Working in a larger model space, both the A3DA and LNPS interactions predict a lower 0_3^+ at 2888 [89] and 2629 keV [93], respectively. The state has a dominant component involving a pair of protons excited out of the $f_{7/2}$ orbital. The deformation of the 0_3^+ state is large, with an intrinsic quadrupole moment around 200 efm^2 ($\beta_2 \sim 0.4$) [95, 97]. A spherical and prolate minimum are also

found on the potential energy surfaces for ^{68}Ni from Hartree-Fock-Bogoliubov theory using the D1SA two-body interaction [99] and a finite range liquid-drop model with microscopic corrections [77]. Experimentally, a state at 2511 keV was initially proposed as the 0_3^+ in β -decay studies [100] and later confirmed using angular correlation analysis [94]. A fourth, low-energy 0^+ state, not expected from a theoretical perspective, was suggested at 2202 keV [95]. However, subsequent analysis of similar reaction data has, so far, failed to support the tentative level [94].

The behavior of the tentative, prolate-deformed 0^+ state in more neutron-rich Ni isotopes beyond $N = 40$ is instructive. Qualitatively different predictions for the continuation of shape coexistence in ^{70}Ni have been offered [77, 97], with only the MCSM calculations suggesting its continued presence [97]. Further, the MCSM calculations suggest the energy of the prolate deformed 0^+ level falls precipitously from 2888 keV in ^{68}Ni to 1525 keV in ^{70}Ni [92]. The drop in the energy of the prolate 0^+ state between ^{68}Ni and ^{70}Ni can be attributed to the role of the tensor component of the monopole interaction, which served to reduce the magnitude of the $Z = 28$ gap as neutrons are added to the $g_{9/2}$ single-particle state. The minimum should be reached at ^{72}Ni and shape coexistence is not predicted to be present in ^{74}Ni [97]. The originally suggested 0_2^+ state at 1484 keV in ^{70}Ni [92] was based on an unplaced γ ray in multinucleon transfer reactions depopulating the 2_1^+ level. The energy of the 0_2^+ has since been corrected following β -decay studies of ^{70}Co and is located at 1567 keV [101].

4.2.2. 2^+ levels Each of the excited 0^+ states in $^{68,70}\text{Ni}$ are predicted to be the lowest member of a rotational band and the 2^+ members are connected to their respective 0^+ states with large $B(E2)$ values [90, 92, 93]. In $^{68,70}\text{Ni}$, there are three 2^+ states connected to the three excited 0^+ levels (two in ^{68}Ni and one in ^{70}Ni) by E2 transitions with large theoretically predicted $B(E2)$ values [90, 92]; see Fig. 8. Unfortunately, in all cases, it is difficult for the low-energy transition, $2_2^+ \rightarrow 0_3^+$ or $2_1^+ \rightarrow 0_2^+$ in ^{68}Ni and $2_2^+ \rightarrow 0_2^+$ in ^{70}Ni to compete with higher-energy deexcitations out of the 2^+ levels to the ground state due to the E_γ^5 dependence on the transition energy. Absolute comparisons of the transition rates with theoretical calculations will have to await future dedicated lifetime experiments, with the exception of the $2_1^+ \rightarrow 0_1^+$ in ^{68}Ni . However, limits on the relative branching ratios out of each state can be converted into relative $B(E2)$ values to compare against theoretical predictions. In ^{70}Ni , the ratio between $B(E2; 2_2^+ \rightarrow 0_2^+)$ to $B(E2; 2_2^+ \rightarrow 0_1^+)$ is predicted to be 4×10^2 from MCSM calculations [92]. Limits on the relative $B(E2)$ values out of individual 2^+ states to their respective 0^+ band members have been determined and compared to theoretical calculations [90] in Fig. 8. More work is needed to identify the low-energy branches for a closer comparison to theory. Other branches not shown in Fig. 8, in particular from the 2_2^+ level, were consistent with shell-model calculations suggesting shape coexistence [93].

4.2.3. Reactions The $^{66}\text{Ni}(t,p)^{68}\text{Ni}$ reaction was performed recently [91] to aid in the interpretation of the nature of 0^+ states [1]. The reaction strongly populates the ground

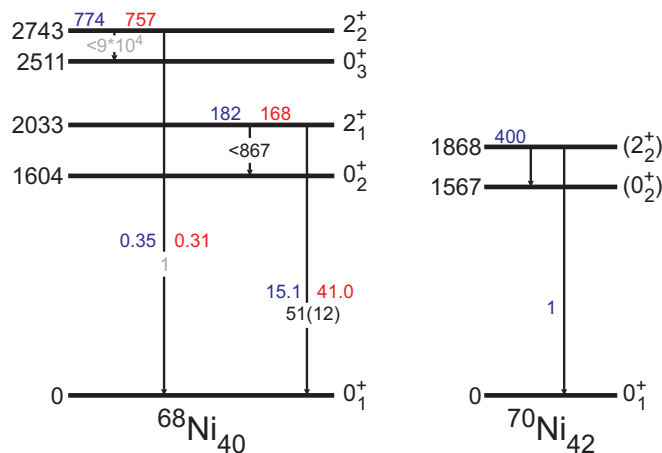


Figure 8. Selected $B(E2)$ values for $^{68,70}\text{Ni}$ taken from [90, 92]. Predictions using the A3DA (LNPS) effective interactions are given in blue (red). Experimental values are given in black. Gray indicates that only relative values out of the indicated state have been measured experimentally. For ^{70}Ni , only the relative $B(E2)$ values were given from the MCSM calculations using the A3DA interaction [92]. Values were taken from Ref. [90] for ^{68}Ni .

state with a weak population to the 0_2^+ states similar to other (t,p) reactions on the lighter Ni isotopes [102]. The results were compared with DWBA cross sections using two-nucleon transfer amplitudes calculated within the shell model using the jj44pna effective interaction [103]. The cross section to the 0_2^+ was reproduced satisfactorily, supporting the notion that this state has a dominant $\nu g_{9/2}^2$ component in agreement with neutron occupancies from other calculations [52, 97]. A mixing analysis between the normal shell model configurations (no excitation into the $\nu g_{9/2}$) and the two-neutron excitation into the $g_{9/2}$ orbital was performed. The results were not conclusive since multiple values for the mixing amplitude between the two states were consistent with the cross section ratio to the 0_1^+ and 0_2^+ states in ^{68}Ni [104]. Transfer reactions with heavier mass beams, such as $^{66}\text{Ni}(^{14}\text{C}, ^{12}\text{C})^{68}\text{Ni}$, may be able to resolve this ambiguity [104]. A small upper limit for the feeding of the 0_3^+ state in ^{68}Ni was observed and is consistent with its expected proton configuration. There is also an unexpectedly strong population to the 2_1^+ state in ^{68}Ni , which was not reproduced by the shell-model calculations and appears very sensitive to the neutron occupancies of the p-orbitals [91].

4.3. The Cu isotopes

The neutron-rich Cu isotopes have one proton outside of the $Z = 28$ shell closure and their low-energy levels should be relatively simple to interpret. At equivalent neutron numbers, the Cu isotopes are easier to access than either Ni or Co and numerous experimental studies have resulted in the systematics presented in Fig. 9 for selected spin-parity states in $^{67,69,71,73,75}\text{Cu}$. Through different experimental probes, the levels in Fig. 9 can be divided into a few classes involving predominately single-particle or

Shape coexistence in neutron-rich nuclei

18

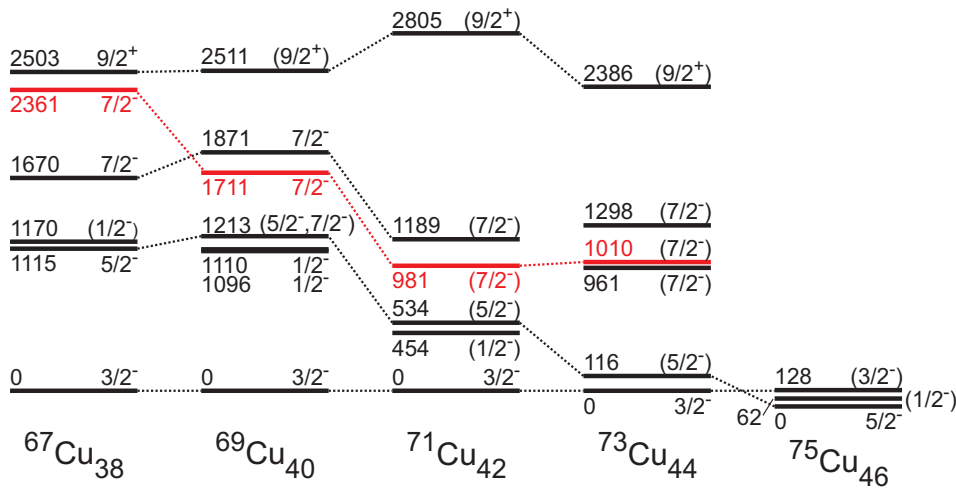


Figure 9. Systematics of selected low-energy states in the Cu isotopes.

collective excitations.

The Cu isotopes from $N = 35$ to 44 have a $3/2^-$ ground state confirmed by in-source and collinear laser spectroscopy [105, 106]. The ground state is attributed to a the single proton in the $p_{3/2}$ orbital. The laser spectroscopy measurements provide not only the spin of the ground states but also their respective g -factors and spectroscopic quadrupole moments. The g -factors at $N = 28$ (^{57}Cu) and $N = 40$ (^{69}Cu) are only slightly below the effective single-particle moment for a pure $p_{3/2}$ configuration. Across the other odd-A Cu isotopes between $N = 30$ to $N = 38$, the experimentally determined g -factor is only slightly below theoretical shell-model calculations employing the $jj44b$ [107] or JUN45 [108] effective interactions in the $f_{5/2}pg_{9/2}$ model space, i.e. excluding excitations across $Z = 28$. The calculations support a dominant single-particle $\pi p_{3/2}$ configuration for the Cu isotopes.

The magnetic moments for the $N = 42, 44$, $3/2^-$ ground states of $^{71, 73}\text{Cu}$, however, fall significantly below the expectations for a pure single-particle configuration and are not reproduced by theoretical calculations which prevent excitations across $Z = 28$. Since magnetic moments are sensitive probes for the orbital occupations of the unpaired nucleon [109], the discrepancy suggests a decreased importance of the $\pi p_{3/2}$ contribution to the ground state wave function in these two nuclei. If the calculations are repeated in a larger model space consisting of the pf shell for protons and $f_{5/2}pg_{9/2}$ for neutrons and allowing for excitations across $Z = 28$, all of the magnetic moments of the odd-A neutron-rich Cu isotopes can be reproduced. Inspection of the calculated wave function indicates the single-particle character of the $3/2^-$ ground state is diminished in $^{71, 73}\text{Cu}$ as the neutron $g_{9/2}$ single-particle orbital is filled [110].

The drop in energy of the first excited ($5/2^-$) state as a function of neutron number is readily apparent in Fig. 9. Assuming that the ($5/2^-$) state can be attributed to the occupation of the $\pi f_{5/2}$ single-particle orbital, a crossing of the $\pi f_{5/2}$ and $\pi p_{3/2}$ orbitals occurs between $N = 44$ and 46. The magnetic moment of ^{75}Cu [105, 106] compared with

theoretical expectations indicate a relatively pure $\pi f_{5/2}$ configuration [110]. The drop in energy of the $(5/2^-)$ state is related to the expected monopole migration of the $\pi f_{5/2}$ orbital [5] due to the strong attractive interaction between the $\pi f_{5/2}$ and $\nu g_{9/2}$ states [106]. Contributions from a proton in the $f_{5/2}$ and neutron in the $g_{9/2}$ single particle states are also inferred from the magnetic moments of the odd-odd 2^- ground states of $^{72,74}\text{Cu}$ [111].

Positive parity states in the odd-A Cu isotopes must originate from an odd number of nucleons promoted into either the proton or neutron positive parity $g_{9/2}$ orbital. A sequence of positive parity $(9/2^+)$ states observed in Fig. 9 is found at a fairly constant excitation energy as a function of neutron number. The $(9/2^+)$ states in lighter odd-A Cu isotopes up to ^{65}Cu carry a large spectroscopic strength in $(^3\text{He},d)$ reactions [112], for example, indicating a large $\pi g_{9/2}$ component in the wave function of these levels. The stability of the $(9/2^+)$ states shown in Fig. 9, with respect to neutron number, argues for their interpretation in terms of a single $\pi g_{9/2}$ weakly coupled to the adjacent Ni, 0^+ ground state. However, some caution is warranted as recent lifetime measurements [113] in ^{67}Cu emphasize the importance of going beyond energy systematics and attribute a more mixed character to the wave function with a $\pi g_{9/2} \otimes J_\nu = 0^+$ component combined with a component of $\pi p_{3/2} \otimes J_\nu = 3^-$ [113].

Contrasting with the near constancy of the $(9/2^+)$ levels in Fig. 9, a separate set of high-spin positive parity states (not presented in Fig. 9) drops down in energy as a function of increasing neutron number [114]. These states can be more closely associated with the coupling of a $p_{3/2}$ proton with negative parity states in the adjacent Ni isotopes. The negative parity states in the even Ni cores necessarily involve excitations into the $g_{9/2}$ orbital. The importance of the $g_{9/2}$ orbital for the positive parity states as neutrons are added to the nucleus is mirrored in the neutron-rich Fe [115] and Mn nuclei [116].

Across the odd-A Cu chain, multiple $(7/2^-)$ states are observed in each isotope. The lowest $(7/2^-)$ states can be grouped into predominately two categories. The first set of $(7/2^-)$ levels are all connected to their respective ground states by large $B(E2; 7/2^- \rightarrow 3/2^-)$ values. These $(7/2^-)$ states roughly follow the excitation energy of the neighboring 2_1^+ states in the Ni isotopes, have $B(E2)$ strengths comparable to the adjacent Ni core, and can be considered as having a configuration dominated by the coupling of the single proton in the $p_{3/2}$ to the 2_1^+ in Ni. Similar comparisons have been made previously in [114, 117]. The other set of $(7/2^-)$ states all have large spectroscopic strength from particle transfer reactions ($\text{Zn}(d, ^3\text{He})$, for example [118]) and are nominally attributed to proton, particle-hole excitations across the $Z = 28$ shell gap. These $(7/2^-)$ states serve as bandheads for sequences of $\Delta J=1$ transitions that have been observed up to spins of at least $15/2^-$ [73, 114, 118, 119]. In $N = 42, 44$ Cu isotopes, the $(7/2^-)$ states still serve as the bandhead for a $\Delta J = 1$ sequence of levels. However, the nature of the state has likely changed from a predominately proton particle-hole excitation to a more collective structure [110] mirroring the trends observed in Ni and Co isotopes at $N = 42$.

The low-energy $(1/2^-)$ levels are also given in Fig. 9. The collective nature of

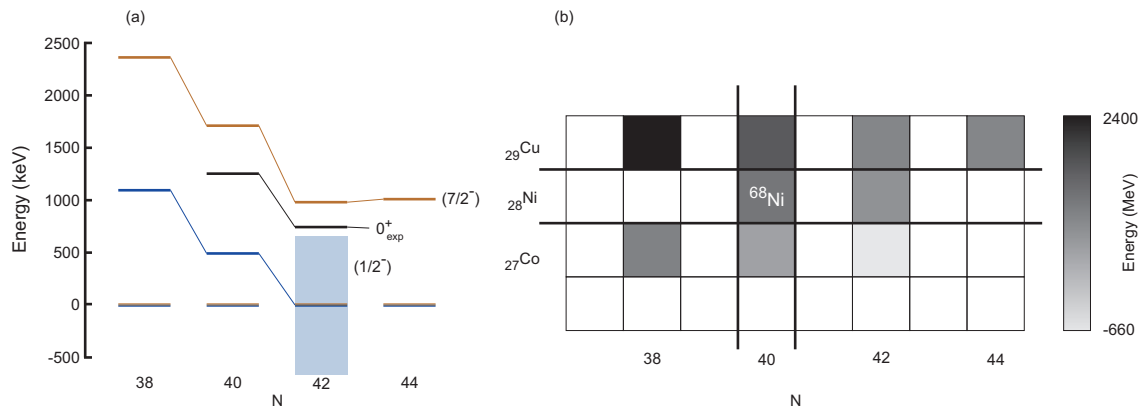


Figure 10. (a) Systematics of the tentatively-identified deformed, intruder $1/2^-$, 0^+ , and $7/2^-$ states in ${}_{27}\text{Co}$ (blue), ${}_{28}\text{Ni}$ (black), and ${}_{29}\text{Cu}$ (copper), respectively. The Ni 0^+ states are divided by two. The shaded area in $N = 42$ represents the range of excitation energies of the the $(1/2^-)$ level with respect to the $(7/2^-)$ in ${}^{69}\text{Co}$. (b) Portion of the chart of nuclides centered on ${}^{68}\text{Ni}$ discussed in this review. The colors show the energy of the deformed intruder configuration relative to the respective ground state. The Ni energies are again divided by a factor of two. The minimum energy of the deformed intruders is currently at $N = 42$, but more experimental work is needed on the more neutron-rich systems at $N = 44$.

the transition between the $(1/2^-)$ level to the $3/2^-$ ground state increases slightly as a function of neutron number experimental with a $B(E2; 1/2^- \rightarrow 3/2^-)$ value of 20.4 W.u. in ${}^{71}\text{Cu}$ and a value of 23.1 W.u. for ${}^{73}\text{Cu}$ [120]. Only a model space which allows for excitations across the $Z = 28$ shell gap can reproduce the energy drop of the $1/2^-$ state as a function of neutron energy [110] and the single-particle proton $p_{3/2}^{+1}$ configuration only accounts for $\sim 30\%$ of the wave function.

4.4. $N = 40$ - The path forward

The systematic trend of the tentatively identified deformed intruder $1/2^-$, 0^+ and $7/2^-$ states in ${}_{27}\text{Co}$, ${}_{28}\text{Ni}$, and ${}_{29}\text{Cu}$, respectively, are collectively presented in Fig. 10. The decrease in the energy of the deformed intruder level is consistent across all three isotopic chains and is expected to reach a minimum around $N = 42$ or 44.

There is still much to do experimentally and theoretically in this region of nuclei to complement the energy systematics shown in Fig. 10. As an example of the complexity of the low-energy level schemes, consider ${}^{70}\text{Ni}$. Within this nucleus will be the expected “normal” single-particle shell-model states, seniority-two states associated with the coupling of the neutrons within the $(g_{9/2})$ to higher total spins and, now, low-energy low-spin deformed intruder states. Differentiating the different types of states will take a large number of complementary experimental approaches. Just a few of the ones that should be undertaken are systematic studies of E0 strengths in neutron-rich Ni isotopes combined with new theoretical approaches for the first-principles derivation of the E0 effective operator [121, 122]. Level-lifetime studies should be undertaken, especially for

the excited 2_1^+ states in even-even Ni nuclei from which absolute $B(E2)$ strengths to the various 0^+ states can be extracted and compared to theory. Reaction measurements are also needed to probe specific components of the nuclear wave functions. Only with all of the measurements can we expect to reach a comprehensive understanding of nuclei in this region, which has been elusive ever since the first spectroscopy studies of ^{68}Ni .

5. Outlook

The future of shape-coexistence studies in neutron-rich nuclei is bright, as new powerful heavy-ion drivers have come into operation in Japan and are under construction in Europe and in the US. Reaction studies that have been employed for decades with stable beams are now being used in inverse kinematics, allowing to access collective and single-particle degrees of freedom in rare isotopes. Advanced detection and digital data acquisition technology continue to push the sensitivity frontiers of in-beam and decay spectroscopy. Progress in the field relies on the close collaboration between experiment and theory, with feedback provided both ways.

Breakthrough measurements have been performed at $N = 20$, $N = 28$ and $N = 40$ recently, establishing and quantifying shape coexistence along these (sub)shell gaps. Many challenges remain for the future, for experiment as well as for theory, promising discoveries and critical insights along these isotone lines that continue to provide key information in the quest for a comprehensive model of nuclear structure and the changes encountered in the regime of large neutron-to-proton asymmetry.

Acknowledgment

This work was partially supported by the National Science Foundation under Grant No. PHY-1102511.

References

- [1] Heyde K and Wood J L 2011 *Rev. Mod. Phys.* **83** 1467
- [2] Warburton E K, Becker J A and Brown B A 1990 *Phys. Rev. C* **41** 1147
- [3] Caurier E, Nowacki F, Poves A and Retamosa J 1998 *Phys. Rev. C* **58** 2033
- [4] Otsuka T, Fujimoto R, Utsuno Y, Brown B A, Honma M and Mizusaki T 2001 *Phys. Rev. Lett.* **87** 082502
- [5] Otsuka T, Suzuki T, Fujimoto R, Grawe H and Akaishi Y 2005 *Phys. Rev. Lett.* **95** 232502
- [6] Zuker A P 1994 *Nucl. Phys. A* **576** 65
- [7] Duflo J and Zuker A P 1999 *Phys. Rev. C* **59** R2347
- [8] Utsuno Y, Otsuka T, Glasmacher T, Mizusaki T, and Honma M 2004 *Phys. Rev. C* **70** 044307
- [9] Thibault C, Klapisch R, Rigaud C, Poskanzer A M, Prieels R, Lessard L and Reisdorf W 1975 *Phys. Rev. C* **12** 644
- [10] Détraz C, Guillemaud D, Huber G, Klapisch R, Langevin M, Naulin F, Thibault C, Carraz L C and Touchard F 1979 *Phys. Rev. C* **19** 164

- [11] Motobayashi T, Ikeda Y, Ieki K, Inoue M, Iwasa N, Kikuchi T, Kurokawa M, Moriya S, Ogawa S, Murakami H, Shimoura S, Yanagisawa Y, Nakamura T, Watanabe Y, Ishihara M, Teranishi T, Okuno H and Casten R 1995 *Phys. Lett. B* **346** 9
- [12] Heyde K and Wood J L 1991 *Journal of Physics G: Nuclear and Particle Physics* **17** 135
- [13] Betz P, Röpke H, Glatz F, Hammel G, Glattes V and Brendler W 1974 *Z. Phys.* **271** 195
- [14] Flynn E, Hansen O, Casten R, Garrett J and Ajzenberg-Selove F 1975 *Nucl. Phys. A* **246** 117
- [15] Wimmer K, Kröll T, Krücken R, Bildstein V, Gernhäuser R, Bastin B, Bree N, Diriken J, Van Duppen P, Huyse M, Patronis N, Vermaelen P, Voulot D, Van de Walle J, Wenander F, Fraile L M, Chapman R, Hadinia B, Orlandi R, Smith J F, Lutter R, Thirolf P G, Labiche M, Blazhev A, Kalkühler M, Reiter P, Seidlitz M, Warr N, Macchiavelli A O, Jeppesen H B, Fiori E, Georgiev G, Schrieder G, Das Gupta S, Lo Bianco G, Nardelli S, Butterworth J, Johansen J and Riisager K 2010 *Phys. Rev. Lett.* **105** 252501
- [16] Rotaru F, Negoita F, Grévy S, Mrazek J, Lukyanov S, Nowacki F, Poves A, Sorlin O, Borcea C, Borcea R, Buta A, Cáceres L, Calinescu S, Chevrier R, Dombrádi Z, Daugas J M, Lehbertz D, Penionzhkevich Y, Petrone C, Sohler D, Stanoiu M and Thomas J C 2012 *Phys. Rev. Lett.* **109** 092503
- [17] Schwerdtfeger W, Thirolf P G, Wimmer K, Habs D, Mach H, Rodriguez T R, Bildstein V, Egido J L, Fraile L M, Gernhäuser R, Hertenberger R, Heyde K, Hoff P, Hübel H, Köster U, Kröll T, Krücken R, Lutter R, Morgan T and Ring P 2009 *Phys. Rev. Lett.* **103** 012501
- [18] Bildstein V, Gernhäuser R, Kröll T, Krücken R, Wimmer K, Van Duppen P, Huyse M, Patronis N and Raabe R 2012 *Eur. Phys. J. A* **48** ISSN 1434
- [19] Rodriguez-Guzman R, Egido J and Robledo L 2002 *Nucl. Phys. A* **709** 201
- [20] Peru, S and Martini, M 2014 *Eur. Phys. J. A* **50**
- [21] Caurier E, Nowacki F and Poves A 2014 *Phys. Rev. C* **90** 014302
- [22] Ibbotson R W, Glasmacher T, Brown B A, Chen L, Chromik M J, Cottle P D, Fauerbach M, Kemper K W, Morrissey D J, Scheit H and Thoennessen M 1998 *Phys. Rev. Lett.* **80** 2081–2084
- [23] Mach H, Fraile L, Tengblad O, Boutami R, Jollet C, Plociennik W, Yordanov D, Stanoiu M, Borge M, Butler P, Cederkall J, Dessagne P, Fogelberg B, Fynbo H, Hoff P, Jokinen A, Korgul A, Kaster U, Kurcewicz W, Marechal F, Motobayashi T, Mrazek J, Neyens G, Nilsson T, Pedersen S, Poves A, Rubio B and Ruchowska E 2005 *The Eur. Phys. J. A* **25** 105
- [24] Niedermaier O, Scheit H, Bildstein V, Boie H, Fitting J, von Hahn R, Köck F, Lauer M, Pal U K, Podlech H, Repnow R, Schwalm D, Alvarez C, Ames F, Bollen G, Emhofer S, Habs D, Kester O, Lutter R, Rudolph K, Pasini M, Thirolf P G, Wolf B H, Eberth J, Gersch G, Hess H, Reiter P, Thelen O, Warr N, Weisshaar D, Aksouh F, Van den Bergh P, Van Duppen P, Huyse M, Ivanov O, Mayet P, Van de Walle J, Äystö J, Butler P A, Cederkäll J, Delahaye P, Fynbo H O U, Fraile L M, Forstner O, Franchoo S, Köster U, Nilsson T, Oinonen M, Sieber T, Wenander F, Pantea M, Richter A, Schrieder G, Simon H, Behrens T, Gernhäuser R, Kröll T, Krücken R, Münch M, Davinson T, Gerl J, Huber G, Hurst A, Iwanicki J, Jonson B, Lieb P, Liljeby L, Schempp A, Scherillo A, Schmidt P and Walter G 2005 *Phys. Rev. Lett.* **94** 172501
- [25] Pritychenko B V, Glasmacher T, Cottle P D, Fauerbach M, Ibbotson R W, Kemper K W, Maddalena V, Navin A, Ronningen R, Sakharuk A, Scheit H and Zelevinsky V 1999 *Phys. Lett. B* **461** 322
- [26] Terry J R, Brown B A, Campbell C M, Cook J M, Davies A D, Dinca D C, Gade A, Glasmacher T, Hansen P G, Sherrill B M, Zwahlen H, Bazin D, Yoneda K, Tostevin J A, Otsuka T, Utsuno Y and Pritychenko B 2008 *Phys. Rev. C* **77** 014316
- [27] Yordanov D T, Bissell M L, Blaum K, De Rydt M, Geppert C, Kowalska M, Krämer J, Kreim K, Krieger A, Lievens P, Neff T, Neugart R, Neyens G, Nörtershäuser W, Sánchez R and Vingerhoets P 2012 *Phys. Rev. Lett.* **108** 042504
- [28] Glasmacher T, Brown B A, Chromik M J, Cottle P D, Fauerbach M, Ibbotson R W, Kemper K W, Morrissey D J, Scheit H, Sklenicka D W and Steiner M 1997 *Phys. Lett. B* **395** 163
- [29] Bastin B, Grévy S, Sohler D, Sorlin O, Dombrádi Z, Achouri N L, Angélique J C, Azaiez F,

- Baiborodin D, Borcea R, Bourgeois C, Buta A, Bürger A, Chapman R, Dalouzy J C, Dlouhy Z, Drouard A, Elekes Z, Franchoo S, Iacob S, Laurent B, Lazar M, Liang X, Liénard E, Mrazek J, Nalpas L, Negoita F, Orr N A, Penionzhkevich Y, Podolyák Z, Pougheon F, Roussel-Chomaz P, Saint-Laurent M G, Stanoiu M, Stefan I, Nowacki F and Poves A 2007 *Phys. Rev. Lett.* **99** 022503
- [30] Reinhard P G, Dean D J, Nazarewicz W, Dobaczewski J, Maruhn J A and Strayer M R 1999 *Phys. Rev. C* **60** 014316
- [31] Rodríguez-Guzmán R, Egido J L and Robledo L M 2002 *Phys. Rev. C* **65** 024304
- [32] Grevy S, Negoita F, Stefan I, Achouri N, Angélique J, Bastin B, Borcea R, Buta A, Daugas J, De Oliveira F, Giarmana O, Jollet C, Laurent B, Lazar M, Liénard E, Marechal F, Mrazek J, Pantelica D, Penionzhkevich Y, Pietri S, Sorlin O, Stanoiu M, Stodel C and St-Laurent M 2005 *Europ. Phys. J. A* **25** 111
- [33] Force C, Grévy S, Gaodefroy L, Sorlin O, Cáceres L, Rotaru F, Mrazek J, Achouri N L, Angélique J C, Azaiez F, Bastin B, Borcea R, Buta A, Daugas J M, Dlouhy Z, Dombrádi Z, De Oliveira F, Negoita F, Penionzhkevich Y, Saint-Laurent M G, Sohler D, Stanoiu M, Stefan I, Stodel C and Nowacki F 2010 *Phys. Rev. Lett.* **105** 102501
- [34] Santiago-Gonzalez D, Wiedenhöver I, Abramkina V, Avila M L, Baugher T, Bazin D, Brown B A, Cottle P D, Gade A, Glasmacher T, Kemper K W, McDaniel S, Rojas A, Ratkiewicz A, Meharchand R, Simpson E C, Tostevin J A, Volya A and Weisshaar D 2011 *Phys. Rev. C* **83** 061305(R)
- [35] Utsuno Y, Shimizu N, Otsuka T, Yoshida T and Tsunoda Y 2015 *Phys. Rev. Lett.* **114** 032501
- [36] Li Z P, Yao J M, Vretenar D, Nikšić T, Chen H and Meng J 2011 *Phys. Rev. C* **84** 054304
- [37] S Peru, M Girod and JF Berger 2000 *Eur. Phys. J. A* **9** 35
- [38] Rodríguez T R and Egido J L 2011 *Phys. Rev. C* **84** 051307
- [39] Sarazin F, Savajols H, Mittag W, Nowacki F, Orr N A, Ren Z, Roussel-Chomaz P, Auger G, Baiborodin D, Belozyorov A V, Borcea C, Caurier E, Dlouhý Z, Gillibert A, Lalleman A S, Lewitowicz M, Lukyanov S M, de Oliveira F, Penionzhkevich Y E, Ridikas D, Sakurai H, Tarasov O and de Vismes A 2000 *Phys. Rev. Lett.* **84** 5062
- [40] Gaodefroy L, Daugas J M, Hass M, Grévy S, Stodel C, Thomas J C, Perrot L, Girod M, Rossé B, Angélique J C, Balabanski D L, Fiori E, Force C, Georgiev G, Kameda D, Kumar V, Lozeva R L, Matea I, Méot V, Morel P, Singh B S N, Nowacki F and Simpson G 2009 *Phys. Rev. Lett.* **102** 092501
- [41] Chevrier R, Daugas J M, Gaodefroy L, Ichikawa Y, Ueno H, Hass M, Haas H, Cottenier S, Aoi N, Asahi K, Balabanski D L, Fukuda N, Furukawa T, Georgiev G, Hayashi H, Iijima H, Inabe N, Inoue T, Ishihara M, Ishii Y, Kameda D, Kubo T, Nanao T, Neyens G, Ohnishi T, Rajabali M M, Suzuki K, Takeda H, Tsuchiya M, Vermeulen N, Watanabe H and Yoshimi A 2012 *Phys. Rev. Lett.* **108** 162501
- [42] Nowacki F and Poves A 2009 *Phys. Rev. C* **79** 014310
- [43] Utsuno Y, Otsuka T, Brown B A, Honma M, Mizusaki T and Shimizu N 2012 *Phys. Rev. C* **86** 051301(R)
- [44] Tostevin J A, Brown B A and Simpson E C 2013 *Phys. Rev. C* **87** 027601
- [45] Fridmann J, Wiedenhöver I, Gade A, Baby L T, Bazin D, Brown B A, Campbell C M, Cook J M, Cottle P D, Diffenderfer E, Dinca D C, Glasmacher T, Hansen P G, Kemper K W, Lecouey J L, Mueller W F, Olliver H, Rodriguez-Vieitez E, Terry J R, Tostevin J A and Yoneda K 2005 *Nature* **435** 922
- [46] Fridmann J, Wiedenhöver I, Gade A, Baby L T, Bazin D, Brown B A, Campbell C M, Cook J M, Cottle P D, Diffenderfer E, Dinca D C, Glasmacher T, Hansen P G, Kemper K W, Lecouey J L, Mueller W F, Rodriguez-Vieitez E, Terry J R, Tostevin J A, Yoneda K and Zwahlen H 2006 *Phys. Rev. C* **74** 034313
- [47] Takeuchi S, Matsushita M, Aoi N, Doornenbal P, Li K, Motobayashi T, Scheit H, Steppenbeck D, Wang H, Baba H, Bazin D, Cáceres L, Crawford H, Fallon P, Gernhäuser R, Gibelin J, Go

- S, Grévy S, Hinke C, Hoffman C R, Hughes R, Ideguchi E, Jenkins D, Kobayashi N, Kondo Y, Krücken R, Le Bleis T, Lee J, Lee G, Matta A, Michimasa S, Nakamura T, Ota S, Petri M, Sako T, Sakurai H, Shimoura S, Steiger K, Takahashi K, Takechi M, Togano Y, Winkler R and Yoneda K 2012 *Phys. Rev. Lett.* **109** 182501
- [48] Baumann T, Amthor A M, Bazin D, Brown B A, Folden C M, Gade A, Ginter T N, Hausmann M, Matos M, Morrissey D J, Portillo M, Schiller A, Sherrill B M, Stolz A, Tarasov O B and Thoennessen M 2007 *Nature* **449** 1022
- [49] Crawford H L, Fallon P, Macchiavelli A O, Clark R M, Brown B A, Tostevin J A, Bazin D, Aoi N, Doornenbal P, Matsushita M, Scheit H, Steppenbeck D, Takeuchi S, Baba H, Campbell C M, Cromaz M, Ideguchi E, Kobayashi N, Kondo Y, Lee G, Lee I Y, Lee J, Li K, Michimasa S, Motobayashi T, Nakamura T, Ota S, Paschalis S, Petri M, Sako T, Sakurai H, Shimoura S, Takechi M, Togano Y, Wang H and Yoneda K 2014 *Phys. Rev. C* **89** 041303
- [50] Tostevin J A, Podolyák G, Brown B A and Hansen P G 2004 *Phys. Rev. C* **70** 064602
- [51] Otsuka T 2013 *Physica Scripta* **2013** 014007
- [52] Lenzi S M, Nowacki F, Poves A and Sieja K 2010 *Phys. Rev. C* **82** 054301
- [53] Shimizu N, Abe T, Tsunoda Y, Utsuno Y, Yoshida T, Mizusaki T, Honma M and Otsuka T 2012 *Prog. Theor. Exp. Phys* **01A205** 27
- [54] Gaudefroy L, Obertelli A, Péru S, Pillet N, Hilaire S, Delaroche J P, Girod M and Libert J 2009 *Phys. Rev. C* **80** 064313
- [55] Bernas M, Dessagne P, Langevin M, Payet J, Pougheon F and Roussel P 1982 *Physics Letters B* **113** 279
- [56] Sorlin O, Leenhardt S, Donzaud C, Duprat J, Azaiez F, Nowacki F, Grawe H, Dombrádi Z, Amorini F, Astier A, Baiborodin D, Belleguic M, Borcea C, Bourgeois C, Cullen D M, Dlouhy Z, Dragulescu E, Górska M, Grévy S, Guillemaud-Mueller D, Hagemann G, Herskind B, Kiener J, Lemmon R, Lewitowicz M, Lukyanov S M, Mayet P, de Oliveira Santos F, Pantalica D, Penionzhkevich Y E, Pougheon F, Poves A, Redon N, Saint-Laurent M G, Scarpaci J A, Sletten G, Stanoiu M, Tarasov O and Theisen C 2002 *Phys. Rev. Lett.* **88** 092501
- [57] Guénaut C, Audi G, Beck D, Blaum K, Bollen G, Delahaye P, Herfurth F, Kellerbauer A, Kluge H J, Libert J, Lunney D, Schwarz S, Schweikhard L and Yazidjian C 2007 *Phys. Rev. C* **75** 044303
- [58] Hannawald M, Kautzsch T, Wöhr A, Walters W B, Kratz K L, Fedoseyev V N, Mishin V I, Böhmer W, Pfeiffer B, Sebastian V, Jading Y, Köster U, Lettry J, Ravn H L and the ISOLDE Collaboration 1999 *Phys. Rev. Lett.* **82** 1391
- [59] Adrich P, Amthor A M, Bazin D, Bowen M D, Brown B A, Campbell C M, Cook J M, Gade A, Galaviz D, Glasmacher T, McDaniel S, Miller D, Obertelli A, Shimbara Y, Siwek K P, Tostevin J A and Weisshaar D 2008 *Phys. Rev. C* **77** 054306
- [60] O Sorlin, C Donzaud, F Nowacki, JC Anglique, F Azaiez, C Bourgeois, V Chiste, Z Dlouhy, S Grvy, D Guillemaud-Mueller, F Ibrahim, K-L Kratz, M Lewitowicz, SM Lukyanov, J Mrasek, Yu-E Penionzhkevich, F de Oliveira Santos, B Pfeiffer, F Pougheon, A Poves, MG Saint-Laurent and M Stanoiu 2003 *Eur. Phys. J. A* **16** 55
- [61] Gade A, Janssens R V F, Baugher T, Bazin D, Brown B A, Carpenter M P, Chiara C J, Deacon A N, Freeman S J, Grinyer G F, Hoffman C R, Kay B P, Kondev F G, Lauritsen T, McDaniel S, Meierbachtol K, Ratkiewicz A, Stroberg S R, Walsh K A, Weisshaar D, Winkler R and Zhu S 2010 *Phys. Rev. C* **81** 051304
- [62] Ljungvall J, Gørgen A, Obertelli A, Korten W, Clément E, de France G, Bürger A, Delaroche J P, Dewald A, Gadea A, Gaudefroy L, Girod M, Hackstein M, Libert J, Mengoni D, Nowacki F, Pissulla T, Poves A, Recchia F, Rejmund M, Rother W, Sahin E, Schmitt C, Shrivastava A, Sieja K, Valiente-Dobón J J, Zell K O and Zielińska M 2010 *Phys. Rev. C* **81** 061301
- [63] Rother W, Dewald A, Iwasaki H, Lenzi S M, Starosta K, Bazin D, Baugher T, Brown B A, Crawford H L, Fransen C, Gade A, Ginter T N, Glasmacher T, Grinyer G F, Hackstein M, Ilie G, Jolie J, McDaniel S, Miller D, Petkov P, Pissulla T, Ratkiewicz A, Ur C A, Voss P, Walsh

- K A, Weisshaar D and Zell K O 2011 *Phys. Rev. Lett.* **106** 022502
- [64] Baugher T, Gade A, Janssens R V F, Lenzi S M, Bazin D, Brown B A, Carpenter M P, Deacon A N, Freeman S J, Glasmacher T, Grinyer G F, Kondev F G, McDaniel S, Poves A, Ratkiewicz A, McCutchan E A, Sharp D K, Stefanescu I, Walsh K A, Weisshaar D and Zhu S 2012 *Phys. Rev. C* **86** 011305
- [65] Crawford H L, Clark R M, Fallon P, Macchiavelli A O, Baugher T, Bazin D, Beausang C W, Berryman J S, Bleuel D L, Campbell C M, Cromaz M, de Angelis G, Gade A, Hughes R O, Lee I Y, Lenzi S M, Nowacki F, Paschalis S, Petri M, Poves A, Ratkiewicz A, Ross T J, Sahin E, Weisshaar D, Wimmer K and Winkler R 2013 *Phys. Rev. Lett.* **110** 242701
- [66] Aoi N, Takeshita E, Suzuki H, Takeuchi S, Ota S, Baba H, Bishop S, Fukui T, Hashimoto Y, Ong H J, Ideguchi E, Ieki K, Imai N, Ishihara M, Iwasaki H, Kanno S, Kondo Y, Kubo T, Kurita K, Kusaka K, Minemura T, Motobayashi T, Nakabayashi T, Nakamura T, Nakao T, Niikura M, Okumura T, Ohnishi T K, Sakurai H, Shimoura S, Sugo R, Suzuki D, Suzuki M K, Tamaki M, Tanaka K, Togano Y and Yamada K 2009 *Phys. Rev. Lett.* **102** 012502
- [67] Freeman S J, Janssens R V F, Brown B A, Carpenter M P, Fischer S M, Hammond N J, Honma M, Lauritsen T, Lister C J, Khoo T L, Mukherjee G, Seweryniak D, Smith J F, Varley B J, Whitehead M and Zhu S 2004 *Phys. Rev. C* **69** 064301
- [68] Block M, Bachelet C, Bollen G, Facina M, Folden C M, Guénaut C, Kwiatkowski A A, Morrissey D J, Pang G K, Prinke A, Ringle R, Savory J, Schury P and Schwarz S 2008 *Phys. Rev. Lett.* **100** 132501
- [69] Lunardi S, Lenzi S M, Della Vedova F, Farnea E, Gadea A, Mărginean N, Bazzacco D, Beghini S, Bizzeti P G, Bizzeti-Sona A M, Bucurescu D, Corradi L, Deacon A N, de Angelis G, Fioretto E, Freeman S J, Ionescu-Bujor M, Iordachescu A, Mason P, Mengoni D, Montagnoli G, Napoli D R, Nowacki F, Orlandi R, Pollarolo G, Recchia F, Scarlassara F, Smith J F, Stefanini A M, Szilner S, Ur C A, Valiente-Dobón J J and Varley B J 2007 *Phys. Rev. C* **76** 034303
- [70] Vermeulen N, Chamoli S K, Daugas J M, Hass M, Balabanski D L, Delaroche J P, de Oliveira-Santos F, Georgiev G, Girod M, Goldring G, Goutte H, Grévy S, Matea I, Morel P, Nara Singh B S, Penionzkevich Y E, Perrot L, Perru O, Péru S, Roig O, Sarazin F, Simpson G S, Sobolev Y, Stefan I, Stodel C, Yordanov D T and Neyens G 2007 *Phys. Rev. C* **75** 051302
- [71] Appelbe D E, Barton C J, Muikku M H, Simpson J, Warner D D, Beausang C W, Caprio M A, Cooper J R, Novak J R, Zamfir N V, Austin R A E, Cameron J A, Malcolmson C, Waddington J C and Xu F R 2003 *Phys. Rev. C* **67** 034309
- [72] Deacon A, Freeman S, Janssens R, Xu F, Carpenter M, Calderin I, Chowdhury P, Hammond N, Lauritsen T, Lister C, Seweryniak D, Smith J, Tabor S, Varley B and Zhu S 2005 *Physics Letters B* **622** 151
- [73] Ishii T, Asai M, Makishima A, Hossain I, Ogawa M, Hasegawa J, Matsuda M and Ichikawa S 2000 *Phys. Rev. Lett.* **84** 39
- [74] Oros-Peusquens A and Mantica P 2000 *Nuclear Physics A* **669** 81
- [75] Pauwels D, Ivanov O, Bree N, Büscher J, Cocolios T E, Gentens J, Huyse M, Korgul A, Kudryavtsev Y, Raabe R, Sawicka M, Stefanescu I, Van de Walle J, Van den Bergh P, Van Duppen P and Walters W B 2008 *Phys. Rev. C* **78** 041307
- [76] Pauwels D, Ivanov O, Bree N, Büscher J, Cocolios T E, Huyse M, Kudryavtsev Y, Raabe R, Sawicka M, Van de Walle J, Van Duppen P, Korgul A, Stefanescu I, Hecht A A, Hoteling N, Wöhr A, Walters W B, Broda R, Fornal B, Krolas W, Pawlat T, Wrzesinski J, Carpenter M P, Janssens R V F, Lauritsen T, Seweryniak D, Zhu S, Stone J R and Wang X 2009 *Phys. Rev. C* **79** 044309
- [77] Möller P, Sierk A, Bengtsson R, Sagawa H and Ichikawa T 2012 *Atomic Data and Nuclear Data Tables* **98** 149
- [78] Recchia F, Lenzi S M, Lunardi S, Farnea E, Gadea A, Mărginean N, Napoli D R, Nowacki F, Poves A, Valiente-Dobón J J, Axiotis M, Aydin S, Bazzacco D, Benzoni G, Bizzeti P G, Bizzeti-Sona A M, Bracco A, Bucurescu D, Caurier E, Corradi L, de Angelis G, Della Vedova F, Fioretto E,

- Gottardo A, Ionescu-Bujor M, Iordachescu A, Leoni S, Mărginean R, Mason P, Menegazzo R, Mengoni D, Million B, Montagnoli G, Orlandi R, Pollarolo G, Sahin E, Scarlassara F, Singh R P, Stefanini A M, Szilner S, Ur C A and Wieland O 2012 *Phys. Rev. C* **85** 064305
- [79] Möller P, Nix J R and Kratz K L 1997 *Atomic Data and Nuclear Data Tables* **66** 131
- [80] Liddick S N, Walters W B, Chiara C J, Janssens R V F, Abromeit B, Ayres A, Bey A, Bingham C R, Carpenter M P, Cartegni L, Chen J, Crawford H L, Darby I G, Grzywacz R, Harker J, Hoffman C R, Ilyushkin S, Kondev F G, Larson N, Madurga M, Miller D, Padgett S, Paulauskas S V, Rajabali M M, Rykaczewski K, Seweryniak D, Suchyta S, and Zhu S 2015 *Phys. Rev. C* **92** 024319
- [81] Liddick S N, Walters W B, Chiara C J, Janssens R V F, Abromeit B, Ayres A, Bey A, Bingham C R, Carpenter M P, Cartegni L, Chen J, Crawford H L, Darby I G, Grzywacz R, Harker J, Hoffman C R, Ilyushkin S, Kondev F G, Larson N, Madurga M, Miller D, Padgett S, Paulauskas S V, Rajabali M M, Rykaczewski K, Seweryniak D, Suchyta S and Zhu S 2015 *Phys. Rev. C* **92** 024319
- [82] Modamio V, Valiente-Dobón J J, Lunardi S, Lenzi S M, Gadea A, Mengoni D, Bazzacco D, Algora A, Bednarczyk P, Benzoni G, Birkenbach B, Bracco A, Bruyneel B, Bürger A, Chavas J, Corradi L, Crespi F C L, de Angelis G, Désesquelles P, de France G, Depalo R, Dewald A, Doncel M, Erduran M N, Farnea E, Fioretto E, Fransen C, Geibel K, Gottardo A, Görgen A, Habermann T, Hackstein M, Hess H, Hüyük T, John P R, Jolie J, Judson D, Jungclaus A, Karkour N, Kempley R, Leoni S, Melon B, Menegazzo R, Michelagnoli C, Mijatović T, Million B, Möller O, Montagnoli G, Montanari D, Nannini A, Napoli D R, Podolyak Z, Pollarolo G, Pullia A, Quintana B, Recchia F, Reiter P, Rosso D, Rother W, Sahin E, Salsac M D, Scarlassara F, Sieja K, Söderström P A, Stefanini A M, Stezowski O, Szilner S, Theisen C, Travers B and Ur C A 2013 *Phys. Rev. C* **88** 044326
- [83] Dijon A, Clément E, de France G, Van Isacker P, Ljungvall J, Görgen A, Obertelli A, Kortén W, Dewald A, Gadea A, Gaodefroy L, Hackstein M, Mengoni D, Pissulla T, Recchia F, Rejmund M, Rother W, Sahin E, Schmitt C, Shrivastava A, Valiente-Dobón J J, Zell K O and Zielińska M 2011 *Phys. Rev. C* **83** 064321
- [84] Carpenter M P, Janssens R V F and Zhu S 2013 *Phys. Rev. C* **87** 041305
- [85] Honma M, Otsuka T, Brown B and Mizusaki T 2005 *The European Physical Journal A - Hadrons and Nuclei* **25** 499
- [86] Ayangeakaa A D, Zhu S, Janssens R V F, Carpenter M P, Albers M, Alcorta M, Baugher T, Bertone P F, Chiara C J, Chowdhury P, David H M, Deacon A N, DiGiovine B, Gade A, Hoffman C R, Kondev F G, Lauritsen T, Lister C J, McCutchan E A, Moerland D S, Nair C, Rogers A M and Seweryniak D 2015 *Phys. Rev. C* **91** 044327
- [87] Albers M, Zhu S, Janssens R V F, Gellanki J, Ragnarsson I, Alcorta M, Baugher T, Bertone P F, Carpenter M P, Chiara C J, Chowdhury P, Deacon A N, Gade A, DiGiovine B, Hoffman C R, Kondev F G, Lauritsen T, Lister C J, McCutchan E A, Moerland D S, Nair C, Rogers A M and Seweryniak D 2013 *Phys. Rev. C* **88** 054314
- [88] Broda R, Pawlat T, Królas W, Janssens R V F, Zhu S, Walters W B, Fornal B, Chiara C J, Carpenter M P, Hotelling N, Iskra L W, Kondev F G, Lauritsen T, Seweryniak D, Stefanescu I, Wang X and Wrzesiński J 2012 *Phys. Rev. C* **86** 064312
- [89] Suchyta S, Liddick S N, Tsunoda Y, Otsuka T, Bennett M B, Chemey A, Honma M, Larson N, Prokop C J, Quinn S J, Shimizu N, Simon A, Spyrou A, Tripathi V, Utsuno Y and VonMoss J M 2014 *Phys. Rev. C* **89** 021301
- [90] Flavigny F, Pauwels D, Radulov D, Darby I J, De Witte H, Diriken J, Fedorov D V, Fedosseev V N, Fraile L M, Huyse M, Ivanov V S, Köster U, Marsh B A, Otsuka T, Popescu L, Raabe R, Seliverstov M D, Shimizu N, Sjödin A M, Tsunoda Y, Van den Bergh P, Van Duppen P, Van de Walle J, Venhart M, Walters W B and Wimmer K 2015 *Phys. Rev. C* **91** 034310
- [91] Elseviers J 2014 Ph.D. thesis KU Leuven
- [92] Chiara C J, Weisshaar D, Janssens R V F, Tsunoda Y, Otsuka T, Harker J L, Walters W B,

- Recchia F, Albers M, Alcorta M, Bader V M, Baugher T, Bazin D, Berryman J S, Bertone P F, Campbell C M, Carpenter M P, Chen J, Crawford H L, David H M, Doherty D T, Gade A, Hoffman C R, Honma M, Kondev F G, Korichi A, Langer C, Larson N, Lauritsen T, Liddick S N, Lunderberg E, Macchiavelli A O, Noji S, Prokop C, Rogers A M, Seweryniak D, Shimizu N, Stroberg S R, Suchyta S, Utsuno Y, Williams S J, Wimmer K and Zhu S 2015 *Phys. Rev. C* **91** 044309
- [93] Recchia F, Chiara C J, Janssens R V F, Weisshaar D, Gade A, Walters W B, Albers M, Alcorta M, Bader V M, Baugher T, Bazin D, Berryman J S, Bertone P F, Brown B A, Campbell C M, Carpenter M P, Chen J, Crawford H L, David H M, Doherty D T, Hoffman C R, Kondev F G, Korichi A, Langer C, Larson N, Lauritsen T, Liddick S N, Lunderberg E, Macchiavelli A O, Noji S, Prokop C, Rogers A M, Seweryniak D, Stroberg S R, Suchyta S, Williams S, Wimmer K and Zhu S 2013 *Phys. Rev. C* **88** 041302
- [94] Chiara C J, Broda R, Walters W B, Janssens R V F, Albers M, Alcorta M, Bertone P F, Carpenter M P, Hoffman C R, Lauritsen T, Rogers A M, Seweryniak D, Zhu S, Kondev F G, Fornal B, Królás W, Wrzesiński J, Larson N, Liddick S N, Prokop C, Suchyta S, David H M and Doherty D T 2012 *Phys. Rev. C* **86** 041304
- [95] Dijon A, Clément E, de France G, de Angelis G, Duchêne G, Dudouet J, Franchoo S, Gadea A, Gottardo A, Hüyük T, Jacquot B, Kusoglu A, Lehbertz D, Lehaut G, Martini M, Napoli D R, Nowacki F, Péru S, Poves A, Recchia F, Redon N, Sahin E, Schmitt C, Sferrazza M, Sieja K, Stezowski O, Valiente-Dobón J J, Vancraeynest A and Zheng Y 2012 *Phys. Rev. C* **85** 031301
- [96] Kaneko K, Hasegawa M, Mizusaki T and Sun Y 2006 *Phys. Rev. C* **74** 024321
- [97] Tsunoda Y, Otsuka T, Shimizu N, Honma M and Utsuno Y 2014 *Phys. Rev. C* **89** 031301
- [98] Pauwels D, Wood J L, Heyde K, Huyse M, Julin R and Van Duppen P 2010 *Phys. Rev. C* **82** 027304
- [99] Girod M, Dessagne P, Bernas M, Langevin M, Pougheon F and Roussel P 1988 *Phys. Rev. C* **37** 2600
- [100] Mueller W F, Bruyneel B, Franchoo S, Huyse M, Kurpeta J, Kruglov K, Kudryavtsev Y, Prasad N V S V, Raabe R, Reusen I, Van Duppen P, Van Roosbroeck J, Vermeeren L, Weissman L, Janas Z, Karny M, Kszczot T, Plochocki A, Kratz K L, Pfeiffer B, Grawe H, Kster U, Thierolf P and Walters W B 2000 *Phys. Rev. C* **61** 054308
- [101] Prokop C J, Crider B P, Liddick S N, Ayangeakaa A D, Carroll J J, Carpenter M P, Chen J, Chiara C J, David H M, Dombos A C, Go S, Grzywacz R, Harker J, Janssens R V F, Larson N, Lauritsen T, Lewis R, Quinn S J, Recchia F, Seweryniak D, Spyrou A, Suchyta S, Walters W B and Zhu S 2015 (submitted)
- [102] Darcey W, Chapman R and Hinds S 1971 *Nuclear Physics A* **170** 253
- [103] Lisetskiy A F, Brown B A, Horoi M and Grawe H 2004 *Phys. Rev. C* **70** 044314
- [104] Lay J A, Fortunato L and Vitturi A 2014 *Phys. Rev. C* **89** 034618
- [105] Vingerhoets P, Flanagan K T, Avgoulea M, Billowes J, Bissell M L, Blaum K, Brown B A, Cheal B, De Rydt M, Forest D H, Geppert C, Honma M, Kowalska M, Krämer J, Krieger A, Mané E, Neugart R, Neyens G, Nörtershäuser W, Otsuka T, Schug M, Stroke H H, Tungate G and Yordanov D T 2010 *Phys. Rev. C* **82** 064311
- [106] Flanagan K T, Vingerhoets P, Avgoulea M, Billowes J, Bissell M L, Blaum K, Cheal B, De Rydt M, Fedosseev V N, Forest D H, Geppert C, Köster U, Kowalska M, Krämer J, Kratz K L, Krieger A, Mané E, Marsh B A, Materna T, Mathieu L, Molkanov P L, Neugart R, Neyens G, Nörtershäuser W, Seliverstov M D, Serot O, Schug M, Sjoedin M A, Stone J R, Stone N J, Stroke H H, Tungate G, Yordanov D T and Volkov Y M 2009 *Phys. Rev. Lett.* **103** 142501
- [107] Cheal B, Mané E, Billowes J, Bissell M L, Blaum K, Brown B A, Charlwood F C, Flanagan K T, Forest D H, Geppert C, Honma M, Jokinen A, Kowalska M, Krieger A, Krämer J, Moore I D, Neugart R, Neyens G, Nörtershäuser W, Schug M, Stroke H H, Vingerhoets P, Yordanov D T and Žáková M 2010 *Phys. Rev. Lett.* **104** 252502
- [108] Honma M, Otsuka T, Mizusaki T and Hjorth-Jensen M 2009 *Phys. Rev. C* **80** 064323

- [109] Neyens G 2003 *Reports on Progress in Physics* **66** 633
- [110] Sieja K and Nowacki F 2010 *Phys. Rev. C* **81** 061303
- [111] Flanagan K T, Vingerhoets P, Bissell M L, Blaum K, Brown B A, Cheal B, De Rydt M, Forest D H, Geppert C, Honma M, Kowalska M, Krämer J, Krieger A, Mané E, Neugart R, Neyens G, Nörtershäuser W, Schug M, Stroke H H and Yordanov D T 2010 *Phys. Rev. C* **82** 041302
- [112] Britton R and Watson D 1976 *Nuclear Physics A* **272** 91
- [113] Niță C R, Bucurescu D, Mărginean N, Avrigeanu M, Bocchi G, Bottoni S, Bracco A, Bruce A M, C ăta Danil G, Coló G, Deleanu D, Filipescu D, Ghiță D G, Glodariu T, Leoni S, Mihai C, Mason P J R, Mărginean R, Negret A, Pantelică D, Podolyak Z, Regan P H, Sava T, Stroe L, Toma S, Ur C A and Wilson E 2014 *Phys. Rev. C* **89** 064314
- [114] Chiara C J, Stefanescu I, Walters W B, Zhu S, Janssens R V F, Carpenter M P, Broda R, Fornal B, Hecht A A, Hoteling N, Jackson E G, Kay B P, Królas W, Lauritsen T, McCutchan E A, Pawlat T, Seweryniak D, Wang X, Wöhr A and Wrzesiński J 2012 *Phys. Rev. C* **85** 024309
- [115] Hoteling N, Chiara C J, Broda R, Walters W B, Janssens R V F, Hjorth-Jensen M, Carpenter M P, Fornal B, Hecht A A, Królas W, Lauritsen T, Pawlat T, Seweryniak D, Wang X, Wöhr A, Wrzesiński J and Zhu S 2010 *Phys. Rev. C* **82** 044305
- [116] Chiara C J, Stefanescu I, Hoteling N, Walters W B, Janssens R V F, Broda R, Carpenter M P, Fornal B, Hecht A A, Królas W, Lauritsen T, Pawlat T, Seweryniak D, Wang X, Wöhr A, Wrzesiński J and Zhu S 2010 *Phys. Rev. C* **82** 054313
- [117] Stefanescu I, Georgiev G, Balabanski D L, Blasi N, Blazhev A, Bree N, Cederkäll J, Cocolios T E, Davinson T, Diriken J, Eberth J, Ekström A, Fedorov D, Fedosseev V N, Fraile L M, Franchoo S, Gladnishki K, Huysse M, Ivanov O, Ivanov V, Iwanicki J, Jolie J, Konstantinopoulos T, Kröll T, Krücken R, Köster U, Lagoyannis A, Lo Bianco G, Maierbeck P, Marsh B A, Napiorkowski P, Patronis N, Pauwels D, Rainovski G, Reiter P, Riisager K, Seliverstov M, Sletten G, Van de Walle J, Van Duppen P, Voulot D, Warr N, Wenander F and Wrzosek K 2008 *Phys. Rev. Lett.* **100** 112502
- [118] Zeidman B and Nolen J A 1978 *Phys. Rev. C* **18** 2122
- [119] Ajzenberg-Selove F, Brown R E, Flynn E R and Sunier J W 1981 *Phys. Rev. C* **24** 1762
- [120] Daugas J M, Faul T, Grawe H, Pfützner M, Grzywacz R, Lewitowicz M, Achouri N L, Angélique J C, Baiborodin D, Bentida R, Béraud R, Borcea C, Bingham C R, Catford W N, Emsallem A, de France G, Grzywacz K L, Lemmon R C, Lopez Jimenez M J, de Oliveira Santos F, Regan P H, Rykaczewski K, Sauvestre J E, Sawicka M, Stanoiu M, Sieja K and Nowacki F 2010 *Phys. Rev. C* **81** 034304
- [121] Bogner S K, Hergert H, Holt J D, Schwenk A, Binder S, Calci A, Langhammer J and Roth R 2014 *Phys. Rev. Lett.* **113** 142501
- [122] Jansen G R, Engel J, Hagen G, Navratil P and Signoracci A 2014 *Phys. Rev. Lett.* **113** 142502